ANALYSIS OF ELECTROMECHANICAL BEHAVIOR OF PIEZOELECTRIC SMART CURVED BEAMS

A Thesis Submitted to
the Graduate School of Engineering and Sciences of
İzmir Institute of Technology
in Partial Fulfillment of the Requirements for the Degree of

MASTER OF SCIENCE

in Mechanical Engineering

by
Tunç ARAS

December 2017
İZMİR

We approve the thesis of **Tunç ARAS name in capital letters**

Examining Committee Members:

Prof. Dr. Bülent YARDIMOĞLU
Department of Mechanical Engineering, İzmir Institute of Technology

Prof. Dr. Serhan ÖZDEMİR
Department of Mechanical Engineering, İzmir Institute of Technology

Prof. Dr. Zeki KIRAL
Department of Mechanical Engineering, Dokuz Eylül University

27 December 2017

Prof. Dr. Bülent YARDIMOĞLU
Supervisor, Department of Mechanical Engineering,
İzmir Institute of Technology

Prof. Dr. Metin TANOĞLU
Head of the Department of
Mechanical Engineering

Prof. Dr. Aysun SOFUOĞLU
Dean of the Graduate School
of Engineering and Sciences

ACKNOWLEDGEMENTS

First, I would like to thank my thesis advisor Prof. Dr. Bülent YARDIMOĞLU for his guidance during this M.Sc. process. He helped me to balance my life after a long military service, encouraged me to finish my studies, and taught me the academic aspect of engineering.

Then, I send my best wishes to my family Ali ARAS and Nalan ARAS. They surrounded me with their love and support. My home will only be a house without them.

Lastly, I would like to thank everyone I shared my life with who is not mentioned above.

ABSTRACT

ANALYSIS OF ELECTROMECHANICAL BEHAVIOR OF PIEZOELECTRIC SMART CURVED BEAMS

In this study, electromechanical behavior of piezoelectric smart curved beam with variable radius of curvature is investigated using Finite Element Method. Firstly, a background of beam theories is provided as well as a discussion on the history of piezoelectric materials and the development of smart beams and smart curved beams. The deformations of curved beams, the differential equations for in-plane bending of curved beam with and without piezoelectric patch are presented. Finite element modeling of smart curved beam is done using ANSYS. The mesh size correctness and numerical accuracy is controlled by an equivalent straight cantilever beam having the same length, cross-section and loaded from its tip with the same amount of force that will be applied to the curved beam model. Tip displacement comparisons are done using an analytical and finite elements approach. The model is verified by comparing the analytical results of piezoelectric constitutive equations with results of finite elements method for a rectangular prism shaped piezoelectric patch. After the verification is complete, the consequent tip displacements on x direction and generated electric fields are observed after the loads of different magnitudes applied to the tip of piezoelectric curved beam. Finally, results are discussed.

ÖZET

PIEZOELEKTRIK AKILLI EĞRI ÇUBUKLARIN ELEKTROMEKANIK DAVRANIŞ ANALIZLERI

Bu çalışmada, değişken eğrilik yarı çaplı akıllı eğri çubukların elektromekanik analizi Sonlu Elemanlar Yöntemi ile incelenmiştir. İlk önce, kiriş teoremleri ve piezoelektrik malzemelerin tarihi ele alınmıştır. Ardından piezoelektrik malzemelerin tarihi, piezoelektrik akıllı çubuk ve akıllı eğri çubukların gelişimi anlatılmıştır. Piezoelektrik eğri çubukların deformasyonu, piezoelektrik bantsız veya bantlı eğri çubukların düzlem içi bükülme diferansiyel denklemleri tanıtılmıştır. Akıllı eğri çubuğun sonlu eleman modellemesi ANSYS ile yapılmıştır. Eğri çubuk ile aynı uzunluğa, keside sahip ve aynı boyutta uç yükle yüklenmiş eş değer düz çubuk ile mesh boyutları ve numerik doğruluğu kontrol edilmiştir.Diktörtgenler prizması şeklindeki piezoelektrik bant için, temel piezoelektrik denklemlerinden sonuçlar ile sonlu elemanlar metodunun sonuçları karşılaştırılarak; model doğrulanmıştır. Doğrulamanın ardından farklı büyüklükteki kuvvetlerin piezoelektrik eğri çubuğa uygulanması sonucunda, çubuk ucundaki x ekseni yönündeki yer değiştirmeler ve oluşturulan elektrik alanlar gözlenmiştir. En sonunda, sonuçlar değerlendirilmiştir.

TABLE OF CONTENTS

LIST OF FIGURES

Figure **Page**

LIST OF TABLES

LIST OF SYMBOLS

a	Coefficient of Archimedean spiral
A	Cross-sectional area of curved beam
b_p	Width of piezoelectric patch
B	Bending rigidity of curved beam
$[B_u]$	Strain-displacement matrix
$[B_V]$	Electrical field-electrical potential matrix
c	Young's modulus (IEEE standard)
$[c]$	Young's modulus matrix
d	Piezoelectric constant without mechanical stress (IEEE standard)
$[d]$	Piezoelectric constant matrix (IEEE standard)
$[d]^T$	Transpose of piezoelectric constant matrix (IEEE standard)
D	Electric displacement (IEEE standard)
$\{D\}$	Dielectric displacement matrix (IEEE standard)
e	Electric displacement and strain relationship (IEEE standard)
$[e]$	Electric displacement and strain relationship matrix (IEEE standard)
$[e]^T$	Transpose of e matrix (IEEE standard)
E	Electric field (IEEE standard)
$\{E\}$	Electric field matrix (IEEE standard)
E_p	Elastic modulus of piezoelectric patch
$\{F\}$	Nodal force vector
h	The moment arm between the centroidal distance of cross-section of curved beam and piezo patch
k	Coupling coefficient of piezoelectric material
l_{xp}	Length of the verification piezoelectric layer
l_{yp}	Height of the verification piezoelectric layer
$[K]$	Structural stiffness matrix
$[K^d]$	Dielectric conductivity
$[K^z]$	Piezoelectric coupling matrix

$[K^z]^T$	Transpose of piezoelectric coupling matrix
L	Length of piezoelectric layer
$\{L\}$	Nodal change vectors
L_p	Length of piezoelectric patch
M_y	Bending moment about y axis
m_y	Distributed bending moment about y axis
N	Internal shear force
N_i	Shape function for node i
$[N^u]$	Shape function matrix for displacements
$[N^u]^T$	Transpose of shape function matrix for displacements
$\{N^V\}$	Shape function matrix for electric potential
$\{N^V\}^T$	Transpose of shape function matrix for displacements
n	Number of disks in the stack
N_i	Shape function for node I
q_n	Distributed internal axial force
q_t	Distributed internal shear force
r	Radius of Archimedean spiral
s	Inverse of Young's modulus (IEEE standard)
$[s]$	Inverse of Young's modulus matrix (IEEE standard)
s^E	s in constant electric field (IEEE standard)
S	Strain (IEEE standard)
$\{S\}$	Strain Matrix (IEEE standard)
t	Thickness of piezoelectric layer
t_p	Thickness of the verification piezoelectric layer
T	Stress (IEEE standard)
T	Internal axial force
$\{T\}$	Stress matrix (IEEE standard)
u	Displacement on curved beam in x direction
w	Displacement on curved beam in z direction
$\{u\}$	Nodal displacement vector
$\{u_c\}$	Displacement vector
U	Voltage (IEEE standard)

$\{V\}$	Nodal electric potential vector
(vol)	Volume
V_c	Electric potential
ΔL	Length change of piezoelectric layer
ε	Strain in s direction
ε	Dielectric constant (IEEE standard)
$[\varepsilon]$	Dielectric constant matrix (IEEE standard)
ε^T	ε in constant stress (IEEE standard)
ε^S	ε in constant strain (IEEE standard)
θ	Polar angle of Archimedean spiral
κ_0'	Initial radius of curvature of curved beam
κ_1'	Deformed radius of curvature of curved beam
ρ_0	Initial radius of curved beam

CHAPTER 1

GENERAL INTRODUCTION

1.1. Introduction

A discussion on the background of beam theories, including the discovery of piezoelectricity and piezoelectric effects and the pioneers who combined piezoelectric effects with beam theories and directly related studies essential to understand the subject of this thesis is provided in the following sections.

1.2. Beam Theories

A beam is a 3D structure (Labuschagne et al. 2009) which has one larger dimension compared to the remaining two. The axis along the larger dimension specifies the beam's axis. It is assumed that the cross-section normal to the axis smoothly changes along the length.

There are many application sites of beams. In civil engineering, there are structures consisting of I, T or square cross-section assembled beams (Bauchau and Craig, 2009a). Many machine parts such as jacks and shafts are also beam-like structures. Furthermore, it is possible to consider aerospace structures of wings and fuselages as thin-walled beams.

Beam Theory is a common and simplified theory referring to beams in solid mechanics. Because of their simplicity in analyzing several structures, they occupy a significant place in structural analysis. Beam models provide significant insight into the behavior of structures. For this reason, they are frequently used in pre-design stages. Their results are also beneficial for validating computational solutions such as finite elements method which is a more sophisticated tool for stress analysis.

Several beam theories were defined based on different assumptions with different levels of accuracies. The first theory, Euler-Bernoulli, dates back to the 18th century (Han et al. 1999). Jacob Bernoulli found out that the curvature of an elastic

beam at any point is proportional to the bending moment of specified point. In later years, Leonhard Euler investigated the shape of elastic beams under different loading conditions and supported the findings of Jacob Bernoulli's. Therefore, the theory is named by joining their surnames. It may also be referred as the Euler beam theory, Bernoulli beam theory or the classical beam theory. Overall, the theory has three assumptions. The cross-section of the beam is infinitely rigid in its plane which allows no deformation. For this reason, in-plane displacement field can be represented by two rigid body translation and one rigid body rotation. Moreover; in case of deformation, the cross-section is assumed to remain plane and normal to the deformed axis. But, experimental results state that these assumptions are only eligible for long, slender beams which have material isotropy. Without those specifications, the Euler-Bernoulli beam theorem becomes inaccurate. Also, the theory overestimates the natural frequencies, especially for higher modes.

The overestimation of natural frequencies in Euler-Bernoulli theorem was attempted to be removed by John William Strutt, 3rd Baron of Rayleigh who added the effect of rotation of the cross-section and he established the Rayleigh Beam Theorem on 1877 (Rayleigh and Lindsay, 1945). While the effect of rotation can be expressed as the angular acceleration of beam elements, this theory gives more satisfying results than Euler-Bernoulli's. However, natural frequencies are still overestimated.

The assumption that the cross-section of the beam remains normal to the deformed axis makes the transverse shear effect disappear in Euler-Bernoulli's theorem. If shear distortion is combined with the bending effect of the Euler-Bernoulli's theorem, Shear Beam theory is reached. Thus, the estimation of natural frequencies improves.

In addition to the theorems mentioned above, Stephen Timoshenko established his own beam theorem by combining the effect of shear and rotation to Euler-Bernoulli's theorem in 1921 and 1922 (Bauchau and Craig, 2009b). Shear or rotary effects are not negligible in this model. Thus, analyses of non-slender beams and its high-frequency responses are improved.

1.3. History of Piezoelectric Materials

After the introduction of beam theories, the foundations of piezoelectric studies and their history should be investigated. The word piezoelectric originates from the Greek words "piezin" which means "to press" and "electron" which has different meanings as “an amber”, “a form of currency”, “a solar divinity” (Olcott, 2013). Before expressing the historical background, phenomena of direct and inverse piezo electric effects illustrated in Figure 1 should be mentioned. The direct piezoelectric effect is generating an electrical charge in proportion to an externally applied force. This effect is used as sensor. However, inverse piezoelectric effect is an expansion of the material due to electric field applied to material and this effect used as actuator.

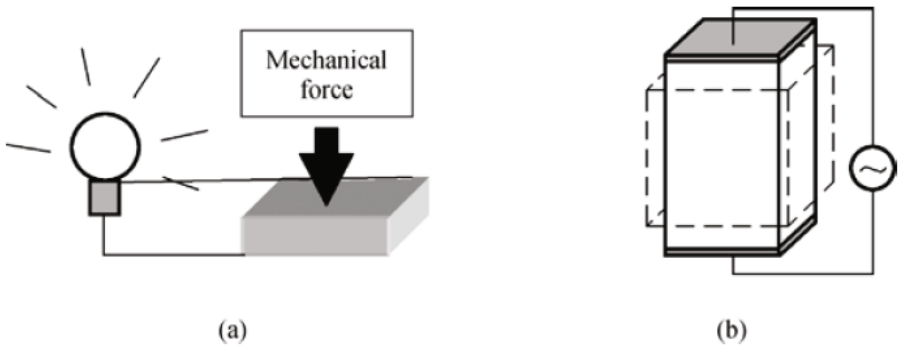

Figure 1.1. Direct and inverse piezoelectric effects: a) Direct effect, b) Inverse effect (Source: Qui 2013)

The Curie brothers, Pierre and Jacques Curie announced direct piezoelectric effect on Academie des Sciences in 2 August 1880 (Gautschi, 2002). This announcement was based on their systematic studies with the crystal symmetry of materials such as zinc blende, sodium chlorate, boracite, tourmaline, cane sugar, rochelle salt and observing their effects. Polar electricity developed due to variations in pressure as a consequence of their experiments. One year later, the inverse piezoelectric effect was predicted by Gabriel Lipmann. He declared that a crystal will deform if an electrical voltage is applied to certain opposite faces of the crystal. On the same year the prediction of Lipmann was confirmed by Curie brothers with their experiments. During their first declaration in 1880, the term piezoelectric was not yet used by Curie brothers. Wilhelm Gottlieb Hankel in 1881 was the first one to propose and the name was immediately accepted in the field (Dineva et al. 2014).

Although the studies by Curie brothers spread to the outside of France and famous scientists of this era such as Woldemar Voigt, Eduard Riecke initiated their own studies of the newly established topic; piezoelectricity remained an object of curiosity instead of practical application for more than 30 years. However, a need for detection of submarines during the First World War changed the situation. Paul Langevin used inverse piezoelectric effect of quartz to create mechanical vibration to emit ultrasonic sound waves underwater. When the created ultrasonic waves were reflected back by objects at the bottom of or in the water, those waves could be captured by same quartz plates before submarines detected by direct piezoelectric effect.

1.4. Developments of Piezoelectric Materials on Smart Beams

Many applications, literatures and patents appeared combining piezoelectric and beam theories after the First World War. But, beam as a word generally represents a line of sound or light in earlier studies. Wente (1922) patented “piezo-electrical voltage indicator” which contained rigidly supported piezoelectric crystalline blades. Seventeen years later, Mason (1939) patented “piezoelectric apparatus and circuits”. He became one of the pioneers who used the word beam as a structural member in piezoelectric applications. These included structures made of low density material, for example aluminum, for weight saving and piezoelectric elements bonded by adhesive material such as shellac. Koren (1949) studied metal strips with thin plate of ceramic soldered on one or both sides which was an early example of active structures for transducer. A combination of piezoelectricity and plate theory was done by Mindlin (1952). Thurston (1953) examined corner loaded, uniformly loaded and central loaded bimorph transducer by theory of elasticity.

Between 1960 and 1970, various patents that contained piezoelectric beams such as piezoelectric ignition system of Crownowner (1966), 3D accelerometer device of Igarashi and Chiku (1967), force transducers of Rogallo (1967) and Norris (1969) were designed. Furthermore, Cain et al. (1967) used transducer to measure the heartbeats of embryo of poultries. Berry (1972) used the forces generated by bending or twisting of piezoelectric material during acceleration and deceleration to design a vehicle speed synthesizer which was intended to be used in antilock brake systems in automobiles. One of the first biomedical application of piezoelectric beam was studied by Williams

and Breger (1975). Rauch and Witter (1976) used a piezoceramic beam for their device that wrote with liquid ink.

The term active structures was established by the 1980's. Also, aerospace applications were initiated. On the other hand, theoretical works appeared. Lee and Marcus (1981) worked on a cantilever mounted piezoelectric bimorph and unimorph structures. Cucci (1982) patented vibrating beam pressure sensor. Bailey and Hubbard (1985) designed and analyzed an active damper for a thin cantilever beam using piezoelectric polymers.

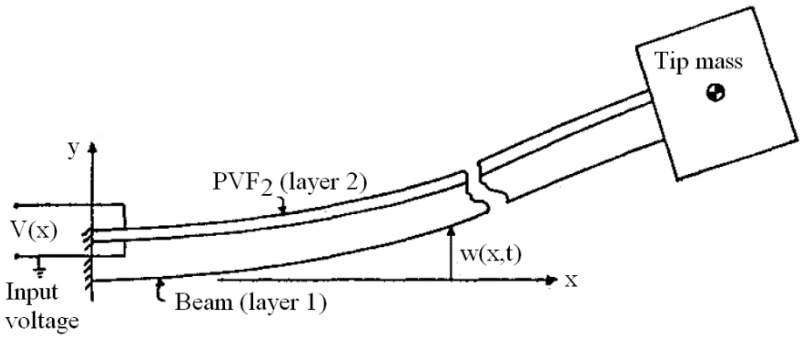

Figure 1.2. Active damper model
(Source: Bailey and Hubbard 1985)

Crawley and De Luis (1987) are the pioneers who used "intelligent structures" by defining them as structures with many actuators, sensors and processing networks. They tested a cantilever beam made of composite and isotropic materials with piezoelectric actuators bonded on them. Tzou (1989) completed various studies such as the development of robot end effector using bimorph. Im and Atluri (1989) investigated the effect of piezoelectric liners on a deformed beam for the usage of model in space structures in which the effect of transverse shear, axial forces and bending moment were investigated.

Tzou and Zhong (1990) simplified the piezoelectric shell to a piezoelectric bimorph cantilever beam. The design, experiments and feasibility of piezoelectric actuators mounted on helicopter blades were accomplished by Hall and Spangler (1990). Lee and Moon (1990) developed modal sensors/actuators for beams and plates.

Studies consisting of smart materials having classical beam models were published during the last decade of 20th century. Inman (1991) finalized his studies between 1987 and 1990 by developing the Timoshenko model of layered piezoelectric devices. Tzou and Howard (1992) extended the studies on smart structures by adding

piezo-thermo elasticity using shell and beam for creating a simplified model. Koconis et al. (1994a) calculated the changes of shape under applied voltage for the fiber reinforced structural elements such as beam, curved beam, rectangular plate with different boundary conditions. Shen (1995) proposed a modeling technique which does not require of integration of piezoelectric devices into the governing equation. Lee (1996) implemented neural network system on smart structures. Lee et al. (1997) concentrated not only on performance of smart material structures, but also their reliability by detailed stress analysis and simulation of crack growth. Aldraihem et al. (1997) compared the Timoshenko and Euler-Bernoulli beam models for suppressing the beam vibration by using piezoelectric sensor and actuator layers. Krommer and Irschik (1999) used laminated beams, plates and shells to investigate the effect of electric field on free transverse vibrations. The study of Wang et al. (1999) was one of the examples which concentrated on sensing capacity of various types of layered beam.

Furthermore, there are remarkable studies published during the late 90's and early 2000's about smart materials with finite element method (hereafter FEM) to be denoted. Söderkvist (1997) used FEM to cope with the difficulty and cost of the experiments of micro-machined structures to obtain the analytical results of piezoelectric cantilever beam. Mackerle (1998) listed all the smart material and structure studies that employed finite element methods between 1986 and 1997. He (2003) expanded his bibliography by adding studies from the same area between 1997 and 2002. Benjeddou (2000) published his research on the piezoelectric adaptive structures modelled by finite elements and concentrating on various specifications such as elements types, their shapes, nodal degree of freedoms, formulations, and assumptions. He also suggested where further developments should be made. Piefort (2001) gave detailed information on his PhD. thesis about history of piezoelectricity, its equations, abilities of different designs, background of finite elements and implementations in smart materials, as well as possible application areas of sensing or actuation capabilities and controlling.

During the first decade of millennium, the number of studies including piezoelectric and beam skyrocketed compared to the previous decade. In fact, there were 427 studies between 1990 and 2000, 1540 from 2000 to 2010 and 2910 in last 7 years from the internet until publishing this thesis. Those values show that the power of the topic has not diminished. Therefore, articles having the highest citations present the trends and developments on smart materials are discussed in the following paragraphs.

As the micro electromechanical systems (hereafter MEMS) became popular, usage of "energy harvesting" from piezoelectric systems instead of external batteries emerged. One of the earlier example was by Elvin et al. (2001). He used a simply supported beam with a strain sensor to generate its power and showed that the frequency and applied force affected the measured strain. Glynne-Jones et al. (2001) showed the voltage generation using a cantilever beam layered with smart materials and carrying mass on tip. The similar study was performed by Lu et al. (2004) using numbers of piezoelectric layers and types. duToit et al. (2005) investigated energy harvesting from vibrations and detailed them for one dimensional harvester model, mass mounted cantilever beam model, harvesting modes and their analytical equations.

Roundy et al. (2005) published a paper on generating more power with vibration based harvesters known as "scavengers" in their research. They concluded that an efficient harvester should have maximum piezoelectric response with respect to the given input, a smaller stress concentration, and also a simple manufacturing method. Moreover, they considered different geometries and boundary conditions, tuning of frequency to enlarge bandwidth, thinner piezoelectric structures, and micro-manufacturing processes which are easily attainable. In the same year, Baker et al (2005) accomplished experimental studies using trapezoid beam for energy harvesting due to showing superiority of trapezoid beam over rectangular beam. They concluded that the output increased 30% and frequency tuning was obtained via bi-stable boundary conditions. Shu and Lien (2006) investigated the optimal power generation for a rectified piezoelectric device. Challa et al. (2008) presented an approach to enlarge the bandwidth of energy harvesting from a cantilever beam that having tip mass between the magnets which reduced the original natural frequency of the system.

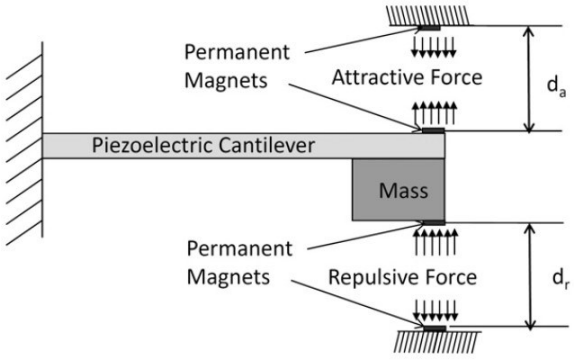

Figure 1.3. Cantilever beam for energy harvesting
(Source: Challa et al. 2008)

In order to correct the past studies, Erturk and Inman (2008) published a new mathematical modeling that considered resonance, true form of piezoelectric coupling and forced vibration terms, true usage of sensing and actuation equations and dynamic deflection patterns. They validated their mathematical model by experimenting a cantilever bimorph beam too (2009). Shen et. al (2008) manufactured a beam with multilayered piezoelectric materials which was in the form of silica wafer for vibration with low frequencies and high amplitudes. Lee et al. (2009) manufactured a composite material by spraying powder of PZT on silica wafer in order to obtain high quality thin piezoelectric film.

Cottone et al. (2009) worked on an inverted pendulum under magnetic excitation at both its base in lateral direction and tip in axial direction. Thus, they proposed a method for stochastic nonlinear oscillators. A similar method was proposed by Ferrari et al. (2010). They used a horizontal cantilever beam instead of an inverted pendulum. The pendulum was excited from its root mechanically, while the tip of it was under magnetic force in the axial direction. Their experimental results showed that the power output increased 88% with respect to linear systems. Also, Stanton et al. (2010) studied nonlinearity concept analytically and experimentally following the former studies. Various bandwidth enlargement techniques were investigated by Tang et al. (2010) according to their advantages and disadvantages. Tabesh and Frenchette (2010) provided energy-harvesting circuit with low power dissipation that was critical for ac/dc voltage conversion.

Wang (2008) was one of the first researcher on usage of nano wires for energy harvesting. The effects of surface stresses of Euler- Bernoulli beam model of nano wires was investigated by Wang and Feng (2010). Sun et al. (2010) tested nano wires statically with different materials and shapes in order to show which generates power the best and generate guideline in future works.

Akaydin et al. (2010) explored energy harvesting from unsteady turbulent fluid flow using piezoelectric generator. On the other hand, Clair et al. (2010) studied an energy harvester based on a cantilever beam subjected to air blow.

Gu and Livermore (2011) presented a double beamed harvester which consisted of one resonant beam that carried mass and one piezoelectric layered beam that vibrates due to impact of mass of the other one. Thus, the system resulted in better power output and increased bandwidth comparing with the conventional one. Zhou et al. (2012)

proposed a cantilever beam with two portions as thick and thin form, namely serially connected. Both portions had mass at the end of them.

Masana and Daqaq (2012) focused on energy harvesting in the super harmonic frequency region of a twin-well (bistable) oscillator. Harne and Wang (2013) concentrated on the mechanical and magnetic bistable systems that generated more power comparing with the linear ones in steady state environment. But their potential was uncertain across the random conditions. Pellegrini et al. (2013) schematically investigated and grouped the bistable harvesters, and summarized nonlinearity, dimensionless effectiveness equations. They stated that the harvesters based on linear oscillators were more effective comparing with the bistable oscillators because of their nonlinear responses despite their high power output capacity.

Li et al. (2014) not only concentrated on conventional beams, but also cymbal type harvesters and curved multilayered harvesters. Zhou et al. (2014) used a model consist of cantilever beam carried two magnet masses on tip. Also, another two extra magnets had optimum position and angle that positioned at right and left side of the tip of the beam. Thus, tri-stability condition was created. Leadenham and Erturk (2014, 2015) designed and experimented a shallow M-shape structure having two inclined bimorph beams as its legs. Those were mounted on two shakers with a proof mass in the middle of the structure to analyze nonlinear energy harvesting for very low base accelerations: primary and secondary resonances.

Cao et al. (2015) also studied the tri-stability condition. He showed how different angles of rested masses at the right side and left side of the beam affected the frequency range and voltage output. Another bi-stable and tri-stable comparison was done by Haitao et al. (2016). However, their beam carried just one magnet on tip.

The daily practical applications of energy harvester became popular due to the developments in that field. Mateu and Moll (2005) studied energy harvesting from daily walking by using various beam shapes with different boundary conditions and alignments. Elvin et al. (2006) focused on civil engineering structures under excitation forces such as traffic, earthquake, and wind for vibration which could be used for structural monitoring based on piezo harvesters.

Anton and Inman (2008) designed a radio controlled UAV (Unmanned Aerial Vehicles) which powered from solar energy and piezoelectricity. They examined the power output of the photovoltaic and piezoelectric devices. Renaud et al. (2009) studied piezoelectric energy harvesting system by motion of human limbs.

Sirohi and Mahadik (2011) proposed a wind energy-harvesting device as an alternate power source. Their system had two parallel cantilever beams with piezoelectric sheets which were attached to a common mass body excited by incident wind. They (2012) also studied a similar topic using a single cantilever beam. Bryant and Garcia (2011) derived a linearized analytical model of a novel piezoelectric energy harvester device driven by flutter vibration of flap pinned at the end of a cantilever beam with piezoelectric patches. Weinstein et al. (2012) used heating, ventilating and air conditioning flow to excite the cantilever beam with piezoelectric energy harvester. Bibo et al. (2015) developed and validated a piezoelectric cantilever-type energy harvester by combining base excitation and aerodynamic forces in their numerical and experimental study.

Li et al. (2013) introduced an acoustic energy harvester that was a quarter-wave length straight-tube acoustic resonator with PVDF piezoelectric cantilever beams placed inside. Bowen and Arafa (2014) summarized the tire pressure monitoring system based on piezoelectric cantilever beams. Cao et al. (2015) used to test the application of bi-stable nonlinear cantilever beam with PZT under magnetic field for power generation from human motion and showed its superiority comparing with the linear and mono-stable harvesters. Wang et al. (2015) theoretically studied energy harvesting from railway systems. Their model was based on Euler-Bernoulli beam on a Winkler foundation. Ansari and Karami (2016) used fan-folded piezoelectric bimorph cantilevers to generate more power from heartbeat vibrations for powering leadless pacemakers.

The general aspects of piezoelectric energy harvesters and a comparison of their models, explanations, and application examples between 2003 and 2006 were reviewed by Anton and Sodano (2007). Another review was published by Khaligh et al. (2010). At their review, Kim et al. (2011) offered a brief explanation in theories and models behind energy harvesting, summarized recently used materials; presented examples of harvesting applications such as usage in shoes, plants and backpacks; explained circuits and storage of harvesters; and offered the future improvements. Wang (2012) reviewed piezoelectric nanogenerators.

Other applications of the piezoelectric beams related with sensing and vibration suppressing were studied by researchers. Lee et al. (2001) used piezoelectric beam for sensing the motion and acceleration in order to investigate the sleep and activity patterns of women diseased by HIV/AIDS. Jean-Louis et al. (2001) used a motion

sensor mounted on the wrist and took accurate results for sensing whether awake and sleeping.

Narayanan and Balamurugan (2003) developed beam, plate, and shell type finite elements for piezoelectric laminates. They also considered the temperature effects in their formulations. Maurini et al. (2004) studied on control of beam vibration by using piezoelectric networks acting as distributed vibration absorbers. Kumar and Narayanan (2008) interested in active vibration control of beams with optimal placement of piezoelectric sensor/actuator pairs.

1.5. Developments of Piezoelectric Material on Smart Curved Beams

Curved beams can be seen in various engineering areas, for example, aerospace, mechanical, civil, etc. Longitudinal axis of curved beam can be two or three dimensional. The simplest planar curve is an arc which has constant radius. However, in some cases, it has variable curvature such as Archimedean spiral.

Two dimensional curved beams can deform in two fashions depending on the load action on it. Those deformations are in-plane and out-of-plane deformations. An in-plane deformation of curved beam has two coupled simple deformations: bending and axial deformation. On the other hand, out-of-plane deformation of curved beam has bending and torsion.

Applications of curved beams and rectangular shaped piezoelectric layers were popular between 1960 and 1980's, such as acoustic transducer modelling and experiments of Royster's (1970), injection pressure measurement device of Heggie (1977) and sandwich curved beam vibration experiment of Vaswani et al (1988).

Designing and modeling semicircular shaped piezoelectric layered curved beams emerged as actuators in the 1990's. The study of Brei and Blechschmidt (1992) was one of the early examples. Three years later, Brei (1995) proposed "C-Block actuators" in the shape of semicircle to be used in different arrangements such as series, arrays, and parallel. He investigated their comparisons with straight beam actuators. Seeley et al (1996) continued to study C-block as offered by Brei to find the hybrid usage of C-blocks in optimum fashion. Moskalik and Brei (1997) presented deflection-voltage model and experimental results for polymeric piezoelectric C-block actuators shown in

Figure 1.4. They (1999) extended their C-block actuator studies to see the force-deflection behavior of the system.

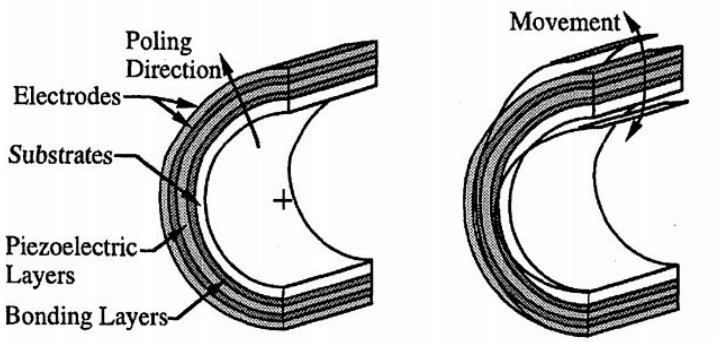

Figure 1.4. Polymeric piezoelectric C-block actuators
(Source: Moskalik and Brei 1997)

Lee (2000) compared straight bimorph actuator and C-block actuator considering their force and displacement output capacities with respect to same amount of given voltage by using finite elements method, and showed that C-Block actuators have advantages in output forces, but disadvantages in output displacements.

Another application area of curved piezoelectric layers is shape controlling. Koconis et al. (1994b) published a highly cited paper on the stated topic. Another shape control application was the study of Saggere and Kota (1999) which included camber shaping of wing structures. Yoon et al. (1998, 2000) examined single and double curved antennas with PZT actuators.

Piezoelectric micro-sensors that embedded on the curved shaped composite structures of ship hulls and planes for structural health monitoring were studied by Krantz et al. (1998, 1999).

Application of the pairing of piezoelectricity and curved beam were widened after 2000. Lobontiu et al. (2001) designed a piezoelectric-driven inchworm locomotion device. Borgen et al. (2003) used two piezoelectric curved beams to design a miniature swimming vehicle. Yoon et al. (2005) developed initially curved piezoelectric unimorph beams with different dimensions under different forces in order to model the energy harvesting from walking. Susanto and Yang (2007) modeled a piezoelectric curved beam actuator for meso/micro grasping. Chen et al. (2008) fabricated a helical actuator designed in ANSYS. Magoteaux et al. (2008) compared the performance differences between UAV without harvester, UAV with curved beam harvester at landing gear, and

UAV with straight beam harvester at landing gear. Results showed that the curved beam harvesters have better power output in high frequencies. Zhou et al. (2010) developed spiral curved beam as a compact energy harvester by using ANSYS. Acoustic energy harvesting from piezoelectric curved beams in the cavity of sonic crystal was studied by Wang et al. (2010). A. Maha and S.-S. Pang (2012) studied on the shape recovery model of a curved beam using piezoelectric actuation. In biomedical area, Kadooka et al. (2015) used multiple connected curved beams in order to create artificial muscle. Yang et al. (2017) compared three energy harvester structures. Those are (i) curved beam in the shape of S connected to straight beam, (ii) C-shaped curved beam connected to straight beam, and (iii) full straight beam. They concluded that the S-shaped curved beam has superiority.

1.6. Aim of the Thesis

In this study, modeling and analyses of curved beams with variable curvature and piezoelectric layer as smart material are studied by using a commercial finite element package that is ANSYS Mechanical. Modeling and solution procedure are coded using APDL (ANSYS Parametric Design Language) in ANSYS. Curved beam is modeled with SOLID45 elements while piezoelectric layer is represented by SOLID5 elements. After validation of the present model, the effects of applied forces to the tip displacement and generated electric field are observed by parametric studies.

CHAPTER 2

THEORETICAL VIBRATION ANALYSIS

2.1. Introduction

In this chapter, the deformations of curved beams are summarized. Based on this section, the differential equations for in-plane bending of the curved beam without piezo patch are presented. Next, the differential equations of curved beam with piezo patch are discussed. Finally, finite element modeling of smart curved beam by using APDL (ANSYS Parametric Design Language) in ANSYS is outlined.

2.2. Geometry of Curved Beams Axis

In order to study a curved beam with variable radius of curvature, an Archimedean spiral $r=a\theta$ is selected for the neutral axis of the curved beam as shown in Figure 2.1.

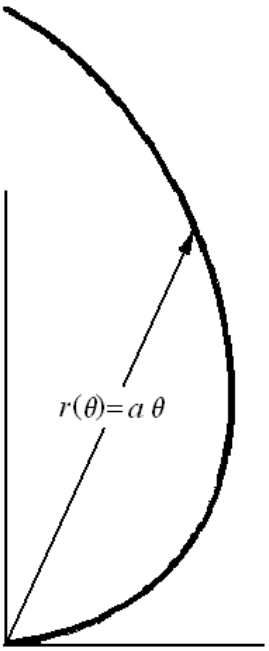

Figure 2.1. Curved beam with variable radius of curvature

2.3. Differential Equations for In-Plane Bending of the Curved Beam

The part of a curved beam with variable radius of curvature and its internal axial force T, internal shear force N, and bending moment M_y about axis y are shown in Figure 2.2. The coordinate system and equations are based on Love (1944).

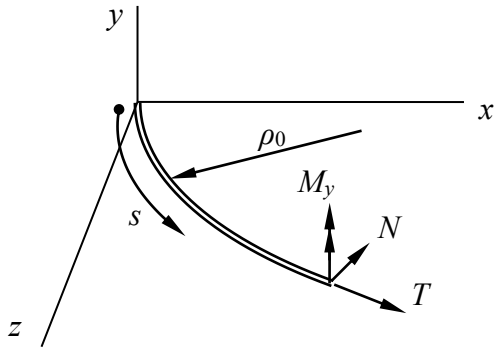

Figure 2.2. A curved beam with variable radius of curvature

The deformed curvature κ_1' in x-z plane is written as

$$\kappa_1' = \kappa_0' + \frac{d}{ds}\left(\frac{du}{ds} + \kappa_0' w\right) \tag{2.1}$$

where u and w are displacements of any point on curved beam in x and z directions, respectively. Also κ_0' is initial curvature. If a curve is represented by for example $r=a\theta$, then curvature is obtained by

$$\kappa_0' = \frac{\left| r^2 + 2\left(\frac{dr}{d\theta}\right)^2 - \frac{d^2 r}{d\theta^2} \right|}{\left[r^2 + \left(\frac{dr}{d\theta}\right)^2 \right]^{3/2}} \tag{2.2}$$

The axial force T is expressed as

$$T = E A \varepsilon \tag{2.3}$$

where ε is strain in direction of s due to tension and given by

$$\varepsilon = \frac{dw}{ds} - \kappa_0' u \tag{2.4}$$

The internal bending moment M_y is expressed as

$$M_y = B(\kappa_1' - \kappa_0') \tag{2.5}$$

where B is original notation used by Love (1944) and represents bending rigidity of curved beam material, which is known as EI.

Equilibrium equations of curved beam for in-plane deformations are written from Love (1944)

$$\frac{dN}{ds} + T\kappa_1' + q_n = 0 \tag{2.6}$$

$$\frac{dT}{ds} - N\kappa_1' + q_t = 0 \tag{2.7}$$

$$\frac{dM_y}{ds} + N + m_y = 0 \tag{2.8}$$

where q_n, q_t are distributed force in normal and tangential directions. Also, m_y is the distributed moment about y axis.

The boundary conditions can be stated as follows:

Either M_y=0 (pinned or free), or w”=0(clamped) (2.9)

Either N=0 (free), or w’=0 (pinned or clamped) (2.10)

Either M_y=0 (pinned or free), or w=0 (pinned or clamped) (2.11)

2.4. Constitutive Equations of Piezoelectric Materials

This section is based on the textbook written by Preumont (2002). The notations of IEEE standard on piezoelectricity (1988) are used in this section. First, one dimensional dielectric medium is presented to discuss the constitutive equation of piezoelectric materials. Then, the three dimensional medium is outlined.

The relationship between the electric field E (V/m) and the electric displacement D (Coulomb/m^2) for an unstressed dielectric medium is given as

$$D = \varepsilon E \tag{2.12}$$

where ε is the dielectric constant or dielectric permittivity (F/m or Coulomb/(Volt×m)) of the material. If elastic body has zero electric field, the relationship between the strain S (-) and the stress T (N/m^2) is written as

$$S = s T \tag{2.13}$$

where s inverse of the Young's modulus of the material which is also called mechanical compliance of the material. Mathematically, s=1/c.

The constitutive equations of a piezoelectric material are related with the mechanical and electrical effects. They are expressed as

$$S = s^E T + d E \tag{2.14}$$

$$D = d T + \varepsilon^T E \tag{2.15}$$

In Equation (2.14), superscript E denotes that the electric field is constant. Also, d (m/V or Coulomb/Newton) is the piezoelectric strain coefficient. In Equation (2.15), superscript T denotes that the stress is constant. Equations (2.14) and (2.15) can be transformed into the following ones

$$T = \frac{1}{s^E} S - \frac{d}{s^E} E \tag{2.16}$$

$$D = \frac{d}{s^E} S + \varepsilon^T \left(1 - \frac{d^2}{s^E \varepsilon^T} \right) E \tag{2.17}$$

Moreover, the last two equations usually expressed as

$$T = c^E S - e E \tag{2.18}$$

$$D = e S + \varepsilon^S E \tag{2.19}$$

where e (Coulomb/m^2) relates the electric displacement with the strain for constant electric field or short-circuited electrodes and expresses as

$$e = d / s^E \tag{2.20}$$

and

$$\varepsilon^S = \varepsilon^T (1 - k^2) \tag{2.21}$$

in which superscript S indicates that the strain is constant and $k^2 = d^2 / (s^E \varepsilon^T)$ is called the coupling coefficient of the piezoelectric material.

The constitutive equations of a three dimensional piezoelectric materials are given in matrix form from Equations (2.14) and (2.15) as follows:

$$\{S\} = [s]\{T\} + [d]\{E\} \tag{2.22}$$

$$\{D\} = [d]^T \{T\} + [\varepsilon]\{E\} \tag{2.23}$$

where superscript T is used to represent the transpose of the matrix. Equations (2.22) and (2.23) are known as actuation and sensing equations of which details are given below:

$$\{S\} = \begin{Bmatrix} S_{11} \\ S_{22} \\ S_{33} \\ 2S_{23} \\ 2S_{31} \\ 2S_{12} \end{Bmatrix} \tag{2.24}$$

$$\{T\} = \begin{Bmatrix} T_{11} \\ T_{22} \\ T_{33} \\ T_{23} \\ T_{31} \\ T_{12} \end{Bmatrix} \tag{2.25}$$

$$\{E\} = \begin{Bmatrix} E_1 \\ E_2 \\ E_3 \end{Bmatrix} \tag{2.26}$$

$$\{D\} = \begin{Bmatrix} D_1 \\ D_2 \\ D_3 \end{Bmatrix} \tag{2.27}$$

$$[s] = \begin{bmatrix} s_{11} & s_{12} & s_{13} & 0 & 0 & 0 \\ s_{12} & s_{22} & s_{23} & 0 & 0 & 0 \\ s_{13} & s_{23} & s_{33} & 0 & 0 & 0 \\ 0 & 0 & 0 & s_{44} & 0 & 0 \\ 0 & 0 & 0 & 0 & s_{55} & 0 \\ 0 & 0 & 0 & 0 & 0 & s_{66} \end{bmatrix} \tag{2.28}$$

$$[d] = \begin{bmatrix} 0 & 0 & d_{31} \\ 0 & 0 & d_{32} \\ 0 & 0 & d_{33} \\ 0 & d_{24} & 0 \\ d_{15} & 0 & 0 \\ 0 & 0 & 0 \end{bmatrix} \tag{2.29}$$

$$[\varepsilon] = \begin{bmatrix} \varepsilon_{11} & 0 & 0 \\ 0 & \varepsilon_{22} & 0 \\ 0 & 0 & \varepsilon_{33} \end{bmatrix} \tag{2.30}$$

The two examples of piezoelectric actuators are shown in Figure 2.3.

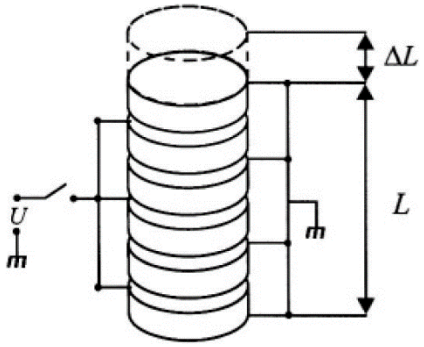

(a) Stacked design

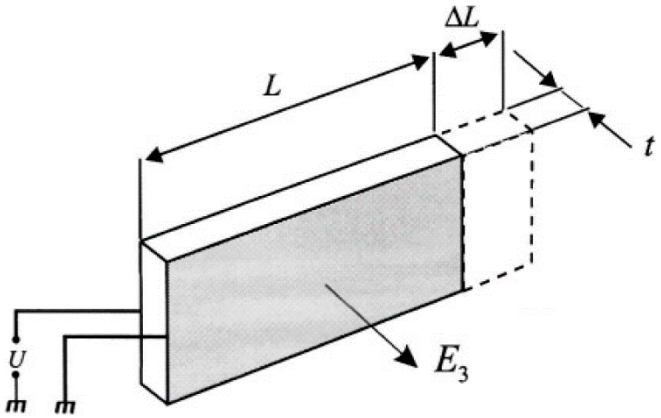

(b) Laminar design

Figure 2.3. The two examples of piezoelectric actuators

The stacked design is related with d_{33}. The change of length due the voltage U applied as shown in Figure 2.3.a is given by

$$\Delta L = d_{33}\, n U \tag{2.31}$$

where n is the number of disks in the stack and U is the applied voltage.

The laminar design is related with d_{31}. The change of length due the voltage U applied as shown in Figure 2.3.b is given by

$$\Delta L = E_3 \, L \, d_{31} \tag{2.32}$$

where

$$E_3 = \frac{U}{t} \tag{2.33}$$

in which U is the applied voltage and t is the thickness of the piezoelectric layer.

2.5. Differential Equations for Smart Curved Beam

The differential equations for in-plane bending of the curved beam with variable curvature are given in Section 2.3 for the applied distributed forces q_n, q_t and distributed moment m_y. If a thin piezoelectric patch is mounted to lateral surface of the curved beam as shown in Figure 2.4 by light gray area, it causes distributed forces in tangential direction which also generates bending moment along the y axis.

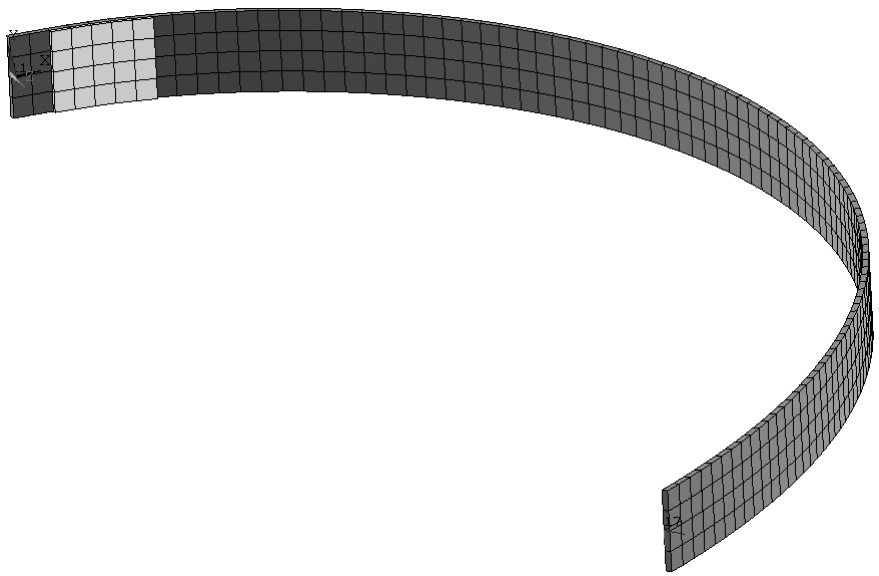

Figure 2.4. Curved beam with piezoelectric patch

Thus, distributed bending moments m_y can be treated in two parts: an externally applied distributed moment denoted by m_{ye} and a distributed moment applied by piezoelectric patch denoted as m_{ye}. The second part can be expressed by using the concentrated moment provided by the textbook written by Preumont (2002) as

$$m_{ye} = E_p \, d_{13} \, b_p \, h U / L_p \tag{2.34}$$

where E_p, b_p and L_p are the Young's modulus, the width and length of the piezoelectric patch. h is the moment arm between the centroidal distance of cross-section of curved beam and piezo patch and U is the applied voltage, respectively.

2.6. Finite Element Modeling of Smart Curved Beam

Equations (2.16) and (2.17) can be written for multidimensional case as follows for finite element formulation (Allik and Hughes, 1970):

$$\{T\} = [c]\{S\} - [e]\{E\} \tag{2.35}$$

$$\{D\} = [e]^T \{S\} + [\varepsilon]\{E\} \tag{2.36}$$

where $\{T\}$ is stress, $\{S\}$ is mechanical strain, $\{E\}$ is electric field, $\{D\}$ is electric flux density vectors. Also, $[c]$, $[e]$, and $[\varepsilon]$ denotes the elastic stiffness matrix evaluated at constant electric field, the piezoelectric matrix and the dielectric matrix evaluated at constant mechanical strain, respectively.

The finite element discretization is accomplished by expressing the field variables in terms of nodal freedoms vector and element shape functions. Therefore, if the nodal displacements vector is denoted by $\{u\}$, the displacements vector $\{u_c\}$ which has the displacements within element in the x, y, z directions is written as (ANSYS, 2004)

$$\{u_c\} = [N^u]^T \{u\} \tag{2.37}$$

where $[N^u]$ is shape function matrix for displacements and given by

$$[N^u] = \begin{bmatrix} N_1 & 0 & 0 & \Lambda & N_n & 0 & 0 \\ 0 & N_1 & 0 & \Lambda & 0 & N_n & 0 \\ 0 & 0 & N_1 & \Lambda & 0 & 0 & N_n \end{bmatrix} \tag{2.38}$$

where the subscript n represents the node number in the finite element. It is useful to express the nodal displacements vector $\{u\}$ in open form

$$\{u\} = \{UX_1 \quad UY_1 \quad UZ_1 \quad \Lambda \quad UX_n \quad UY_n \quad UZ_n\}^T \tag{2.39}$$

Similarly, if the nodal electrical potential vector is denoted by $\{V\}$, the electrical potential V_c within element is written as (ANSYS, 2004)

$$V_c = \{N^V\}^T \{V\} \tag{2.40}$$

where $\{N^V\}$ is shape function vector of electrical potential shape function and given by

$$\{N^V\}^T = \begin{pmatrix} N_1 & N_2 & \Lambda & N_n \end{pmatrix} \tag{2.41}$$

in which N_i is the shape function for node i. Again, it is useful to express the nodal electrical potential vector $\{V\}$ in open form as

$$\{V\} = \{V_1 \quad V_2 \quad \Lambda \quad V_n\}^T \tag{2.42}$$

The strain vector $\{S\}$ is related to the displacement vector $\{u\}$ as

$$\{S\} = [B_u]\{u\} \tag{2.43}$$

where $[B_u]$ is written as

$$[B_u] = \begin{bmatrix} \frac{\partial}{\partial x} & 0 & 0 \\ 0 & \frac{\partial}{\partial y} & 0 \\ 0 & 0 & \frac{\partial}{\partial z} \\ \frac{\partial}{\partial y} & \frac{\partial}{\partial x} & 0 \\ 0 & \frac{\partial}{\partial z} & \frac{\partial}{\partial y} \\ \frac{\partial}{\partial z} & 0 & \frac{\partial}{\partial x} \end{bmatrix} \tag{2.44}$$

On the other hand, the electric field vector {E} is related to the electrical potential vector $\{V\}$ as

$$\{E\} = -[B_V]\{V\} \tag{2.45}$$

where $[B_V]$ is written as

$$[B_V] = \begin{Bmatrix} \frac{\partial}{\partial x} \\ \frac{\partial}{\partial y} \\ \frac{\partial}{\partial z} \end{Bmatrix} \{N^V\}^T \tag{2.46}$$

The coupled finite element matrix equation is obtained using the Equations (2.37) to (2.46) in the variational principle available in the paper of Allik and Hughes (1970) and expressed for static problem by using the notation in ANSYS (2004) as

$$\begin{bmatrix} [K] & [K^z] \\ [K^z]^T & [K^d] \end{bmatrix} \begin{Bmatrix} \{u\} \\ \{V\} \end{Bmatrix} = \begin{Bmatrix} \{F\} \\ \{L\} \end{Bmatrix} \tag{2.47}$$

where $[K]$, $[K^d]$, and $[K^z]$ are structural stiffness, dielectric conductivity, and piezoelectric coupling matrices, respectively. $\{F\}$ and $\{L\}$ are nodal force and nodal charge vectors, respectively. They are given in ANSYS (2004) as

$$[K] = \int_{vol} [B_u]^T [c][B_u] d(vol) \tag{2.48}$$

$$[K^d] = \int_{vol} [B_V]^T [\varepsilon][B_V] d(vol) \tag{2.49}$$

$$[K^z] = \int_{vol} [B_u]^T [e][B_V] d(vol) \tag{2.50}$$

After finding the nodal displacement and electric potential for an element, stresses and electric flux density at any point within the finite element can be obtained by substituting Equations (2.43) and (2.45) into Equations (2.35) and (2.36) as

$$\{T\} = [c][B_u]\{u\} + [e][B_V]\{V\} \tag{2.51}$$

$$\{D\} = [e]^T [B_u]\{u\} - [\varepsilon][B_V]\{V\} \tag{2.52}$$

The finite element model of the smart curved beam with variable curvature is generated in ANSYS by using SOLID45 and SOLID5 for beam and piezoelectric patch, respectively. A computer code in ANSYS is developed by using APDL (ANSYS Parametric Design Language).

CHAPTER 3

NUMERICAL RESULTS AND DISCUSSION

3.1. Validation of Model

The axis of the curved beam with the equation $r=4\theta$, ($0^o< \theta < 90^o$) is generated in ANSYS by using a spline that fits to a series of 50 keypoints. The length of the axis is s=476.5 mm. Cross-section of the beam with b=20 mm and h=1.5 mm is dragged along the spline in order to form the volume. Fixed-free boundary conditions are used. Several numbers of elements to mesh the curved beam are used to have the theoretical tip displacement due to the load acting on tip and then element size in axial, tangential and radial directions are decided as 5 mm, 4.9635 mm, and 1.5 mm, respectively. Details are presented in this section. The meshed curved beam is shown in Figure 3.1.

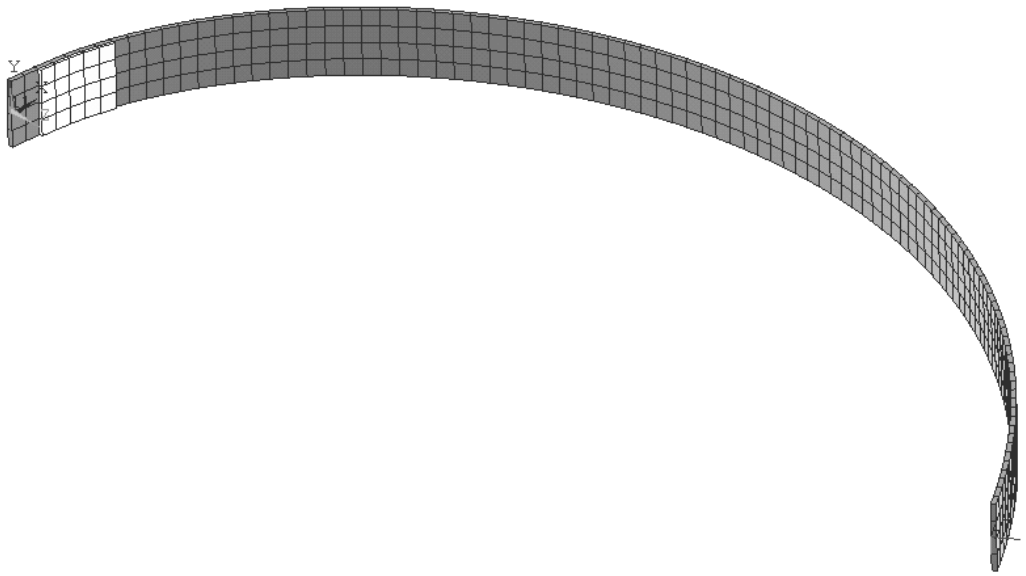

Figure 3.1 The curved beam and smart patch as meshed

The piezoelectric layer with b_p=20 mm, s_p=25 mm, and t_p=1 mm is bonded to concave surface of the curved beam at the distance d_p=10 mm from the root. Its mesh is shown in Figure 3.1 by light grey color.

The material properties of curved beam and piezoelectric layer given in Tables 3.1 and 3.2, respectively, are taken from Malgaca (2007).

Table 3.1. Material Properties of curved beam

Material	Aluminum
Young modulus (N/m^2)	$62\ 10^9$
Density (kg/m^3)	2676
Poisson's ratio	0.32

Table 3.2. Material Properties of piezoelectric layer

Material	BM532 (PZT-5H)
c_{11} (N/m^2)	$12.6\ 10^{10}$
c_{12} (N/m^2)	$7.95\ 10^{10}$
c_{13} (N/m^2)	$8.41\ 10^{10}$
c_{33} (N/m^2)	$11.7\ 10^{10}$
c_{44} (N/m^2)	$2.33\ 10^{10}$
e_{31} (C/m^2)	-6.5
e_{33} (C/m^2)	23.3
e_{25} (C/m^2)	17
ε_{11} (F/m)	$1.503\ 10^{-8}$
ε_{22} (F/m)	$1.503\ 10^{-8}$
ε_{33} (F/m)	$1.3\ 10^{-8}$

The material data given in Table 3.1 and 3.2 are coded in APDL by using the following lines:

```
mp,ex,1,62e9                ! Young modulus of aluminum
mp,dens,1,2676              ! Density of aluminum
mp,nuxy,1,0.32              ! Poisson's ratio of aluminum
```

```
mp,dens,2,7350                  ! Density of PZT
mp,perx,2,15.03e-9              ! epsilon11
mp,pery,2,15.03e-9              ! epsilon22
mp,perz,2,13e-9                 ! epsilon33
tb,piez,2                       ! Table of e for PZT
tbdata,3,-6.5                   ! e31
tbdata,6,-6.5                   ! e32
tbdata,9,23.3                   ! e33
tbdata,14,17                    ! e25
tbdata,16,17                    ! e16
tb,anel,2                       ! Table of c for PZT
tbdata,1,126e9,79.5e9,84.1e9    ! c11, c12, c13
tbdata,7,126e9,84.1e9           ! c22, c23
tbdata,12,117e9                 ! c33
tbdata,16,23.25e9               ! c44
tbdata,19,23e9                  ! c55
tbdata,21,23e9                  ! c66
```

In order to present the correctness and numerical accuracy of the finite element model of the beam without piezoelectric layer due to mesh size selection, an equivalent straight cantilever beam having the same length and cross-section is loaded from its tip by 0.5 N. Then, the tip displacement of the cantilever beam is found from analytical method and finite element model. The results are given in Table 3.3.

Table 3.3. Tip displacements of cantilever beam (m)

Analytical	0.0517
Numerical by FEM	0.0514

The difference between analytical and numeric result is 0.580271%. Thus, it can be concluded from Table 3.3 that the present finite element model gives satisfactory result based on the mesh distribution used to model the beam.

The analytical solution for the curved beam with piezoelectric layer in the selected geometry is not available in the existing literature. Therefore, the piezoelectric layer in the form of thin rectangular prism with l_{xp}=25 mm, l_{yp}=20 mm, and t_p=1 mm is fixed left hand and loaded from the right hand as shown in Figure 3.2 in order to validate finite element model of the laminar form of piezoelectric layer. Although, the piezoelectric layer is bonded concave side of curved beam by adopting its curvature, the curvature of the piezoelectric layer is neglected in this validation to compare the numerical results with analytical results obtained from Equation (2.22).

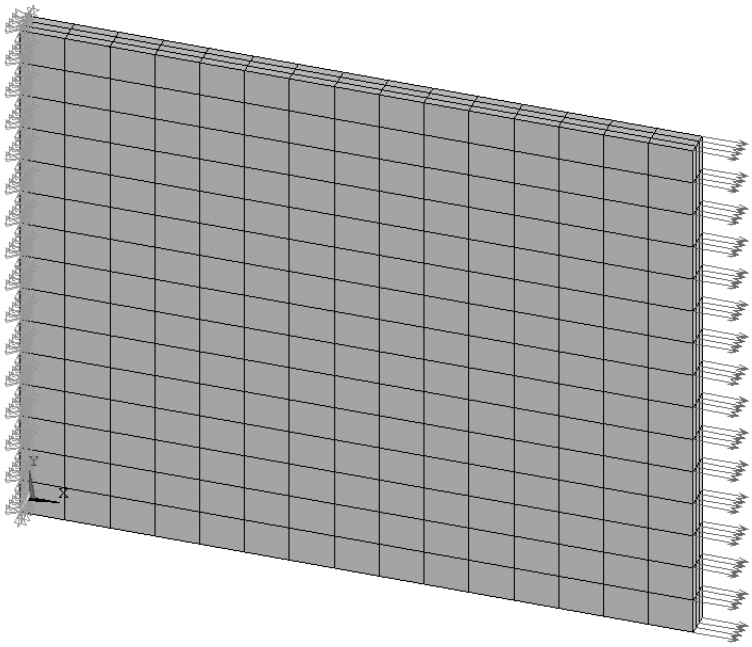

Figure 3.2. The finite element model of piezoelectric layer

Analytical results are calculated by using E_3=-2 10^5 Volt/m and T_1=25 10^5 N/m^2. Other data for PZT-5H are s_{11}^E=16.5 10^{-12} m^2/N and d_{13}=-274 10^{-12} C/N. Thus,

- Strain in x direction due to stress acting in x direction is equal to $s_{11}^E T_1$=0.413 10^{-4}.
- Strain in x direction due to electric field in z direction is equal to $d_{11}^E E_3$=0.548 10^{-4}.
- Strain in x direction due to stress acting in x direction and electric field applied in z direction is equal to $S_1=s_{11}^E T_1+ d_{11}^E E_3$=0.961 10^{-4}.

Finite element model results are given in Figures 3.3-3.5 in the same order of the analytical results presented above.

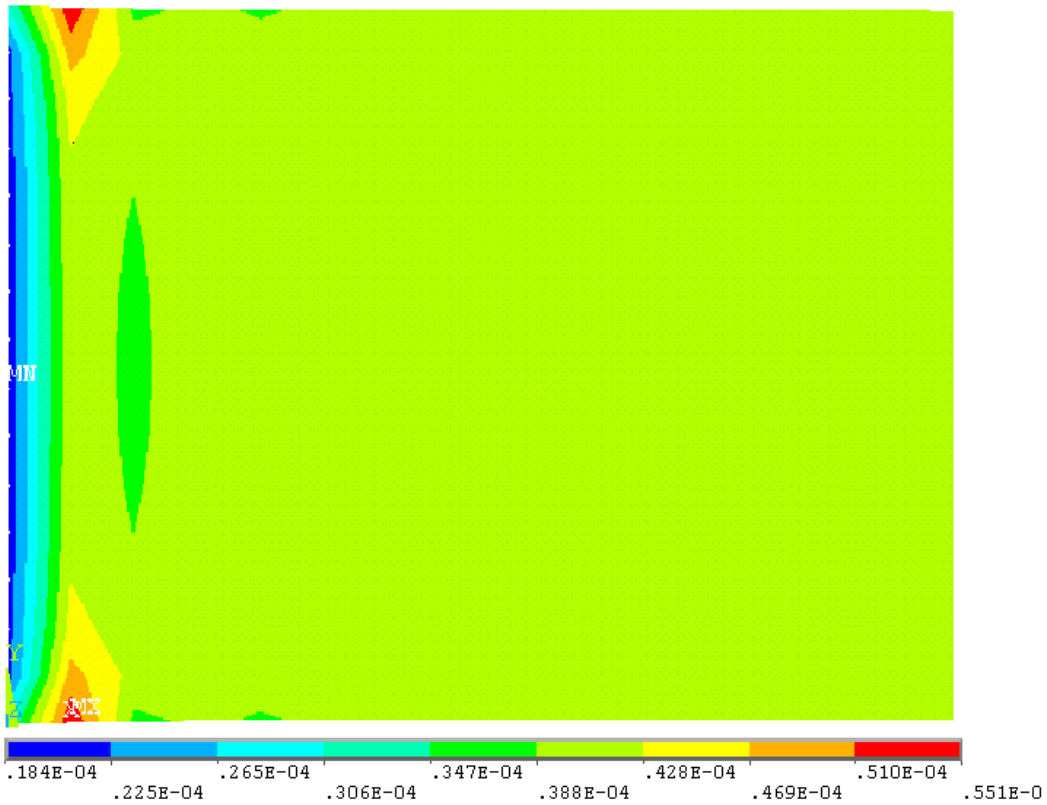

Figure 3.3. Strain in *x* direction due to force applied in *x* direction

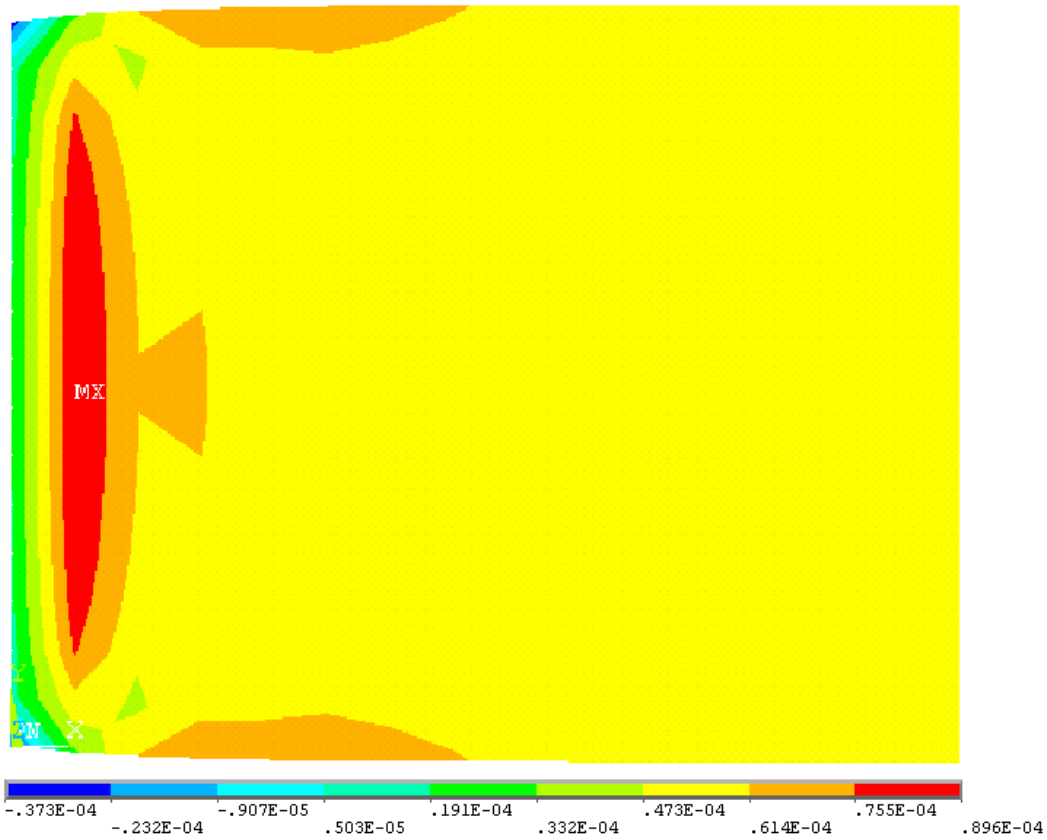

Figure 3.4. Strain in *x* direction due to voltage applied in *z* direction

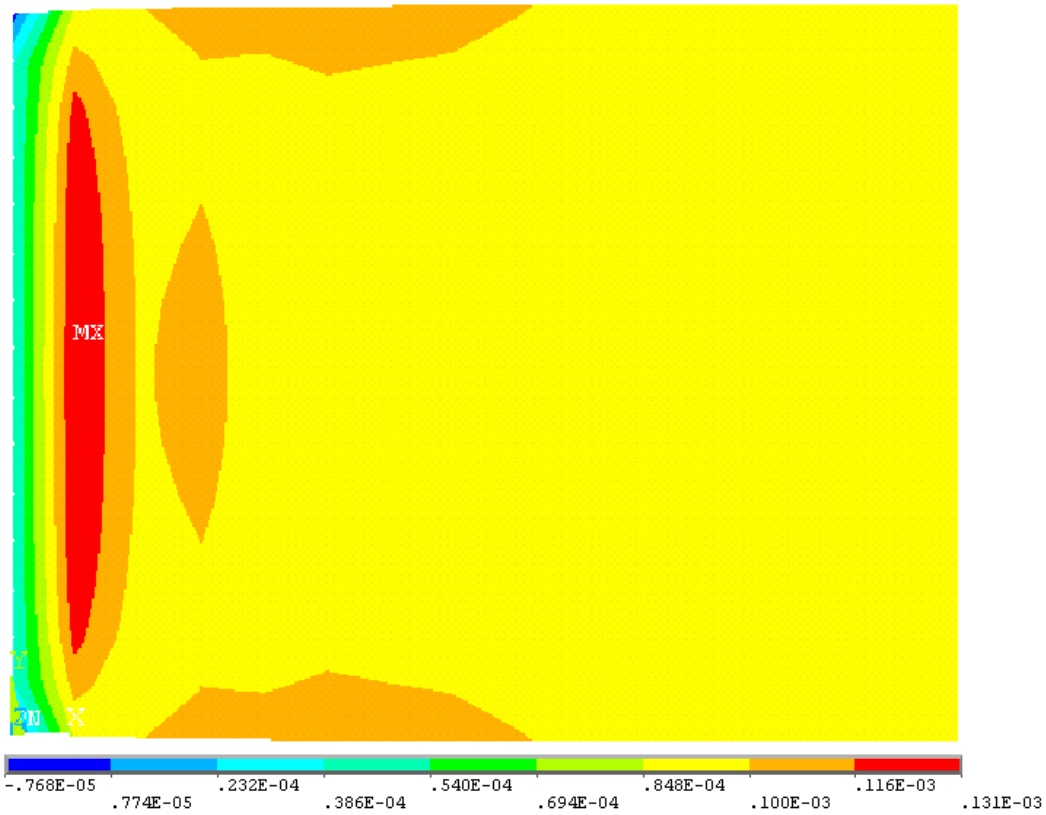

Figure 3.5. Strain in *x* direction due force and voltage

When the Figures 3.3-3.5 are examined, the following validations can be said:

- Strain in *x* direction due to stress acting in *x* direction is generally shown by the color of which scale is the fourth part from the right. It has an interval [0.388E-04, 0.428E-04]. The analytical result 0.413 10^{-4} is in this interval.
- Strain in *x* direction due to electric field in *z* direction is generally shown by the color of which scale is the third part from the right. It has an interval [0.473E-04, 0.614E-04]. The analytical result 0.548 10^{-4} is in this interval.
- Strain in *x* direction due to stress acting in *x* direction and electric field applied in *z* direction is generally shown by the color of which scale is the third part from the right. It has an interval [0.848E-04, 1.000E-03]. The analytical result 0.961 10^{-4} is in this interval.

Therefore, the finite element model of piezoelectric layer is proven.

3.2. Analysis with Present Model

The curved beam model described Section 3.1 illustrates an electromechanical model of curved beam with piezoelectric layer bonded to concave side of the curved beam as a patch. The voltage generation of the bonded piezoelectric layer due to the load acting on tip of the curved beam is the main topic in this study. The tip load is selected as 0.1 N and 0.5 N in the analysis.

In order to see the in-plane displacements of the curved beam under the tip load acting in plane of the neutral axis of the curved beam, deformed and undeformed states of the respective system are illustrated in Figure 3.6 and Figure 3.11 for tip load 0.1 N and 0.5 N, respectively. Displacements of the tip of the curved beam in *x* direction can be read from aforementioned figures as 0.00562 mm and 0.028101 mm for tip load 0.1 N and 0.5 N, respectively. Results indicate that displacements are linearly proportional to tip load as expected from the linear elasticity.

Electrical fields generated by strains in piezoelectric layer due to the tip load 0.1 N are shown for entire curved beam in Figure 3.7 and for PZT layer in Figure 3.8. Also, Figure 3.12 and Figure 3.13 are counterparts of Figures 3.7 and Figure 3.8 for tip load 0.5 N. Maximum values of electrical field in Figure 3.8 and Figure 3.9 are 10354 V/m and 51771 V/m, respectively. They show that electrical field linearly proportional to tip load again as expected from the theory.

Strains of PZT layer in *x* direction due to tip load 0.1 N and 0.5 N are shown in Figure 3.9 and Figure 3.14, respectively. The reason for selecting direction of *x* only is the 31 operating mode of piezo patch. Maximum strain values in PZT layer in *x* direction which is related with operating mode 31 from related figures are found as follows: 0.223E-04 for 0.1 N, 0.111E-03 for 0.5 N. The numerical values are proportional to each other.

Moreover, in order to check the stress levels of the curved beam due to the tip load, stress contours in root region of curved beam and PZT layer are presented in Figure 3.10 and Figure 3.15 for tip load 0.1 N and 0.5 N, respectively. Maximum stress values in PZT layer in *x* direction as follows: 0.169E+07 Pa for 0.1 N, 0.845E+07 Pa for 0.5 N. The numerical values are proportional to each other.

The mentioned values can be seen from the figures below, where the numbers below the figures increases from left to right.

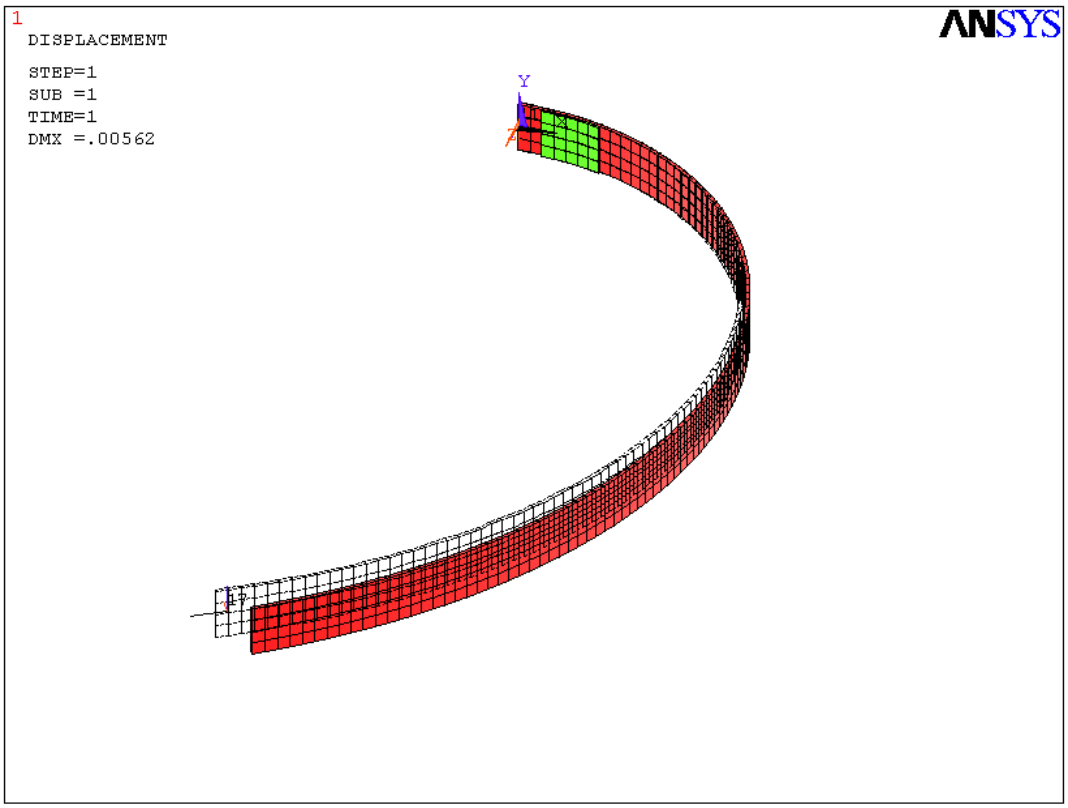

Figure 3.6. Deformed and undeformed states of curved beam under tip load 0.1 N

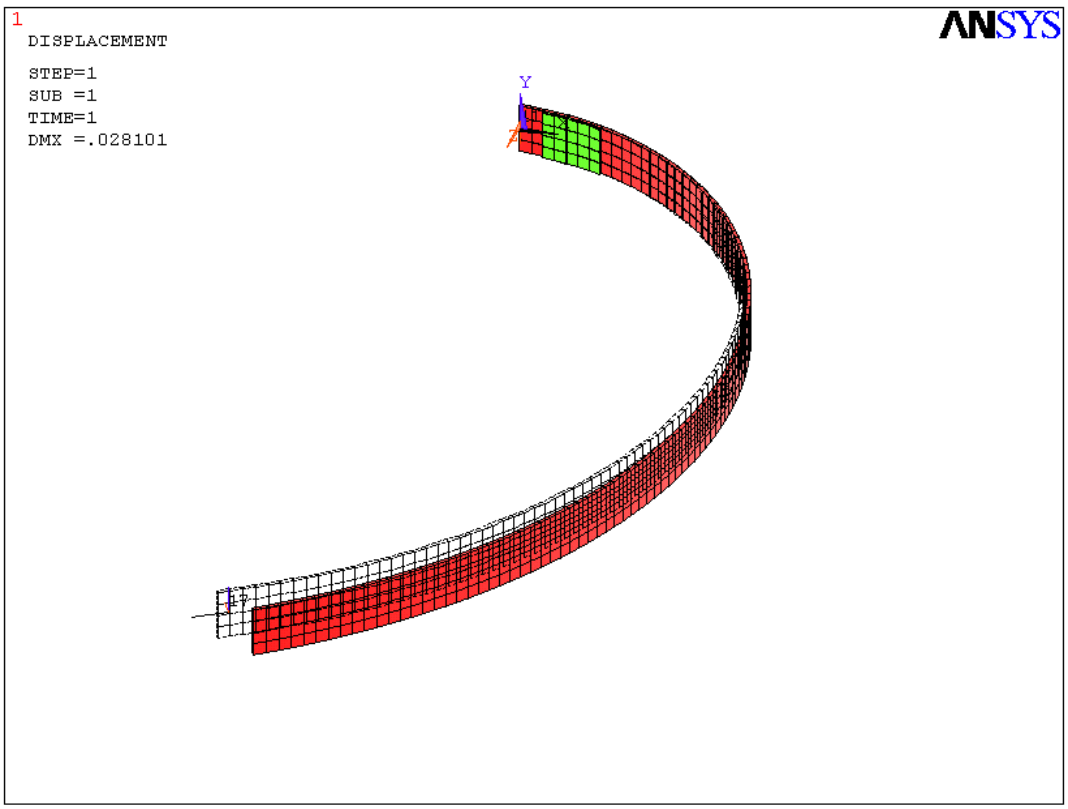

Figure 3.7. Deformed and undeformed states of curved beam under tip load 0.5 N

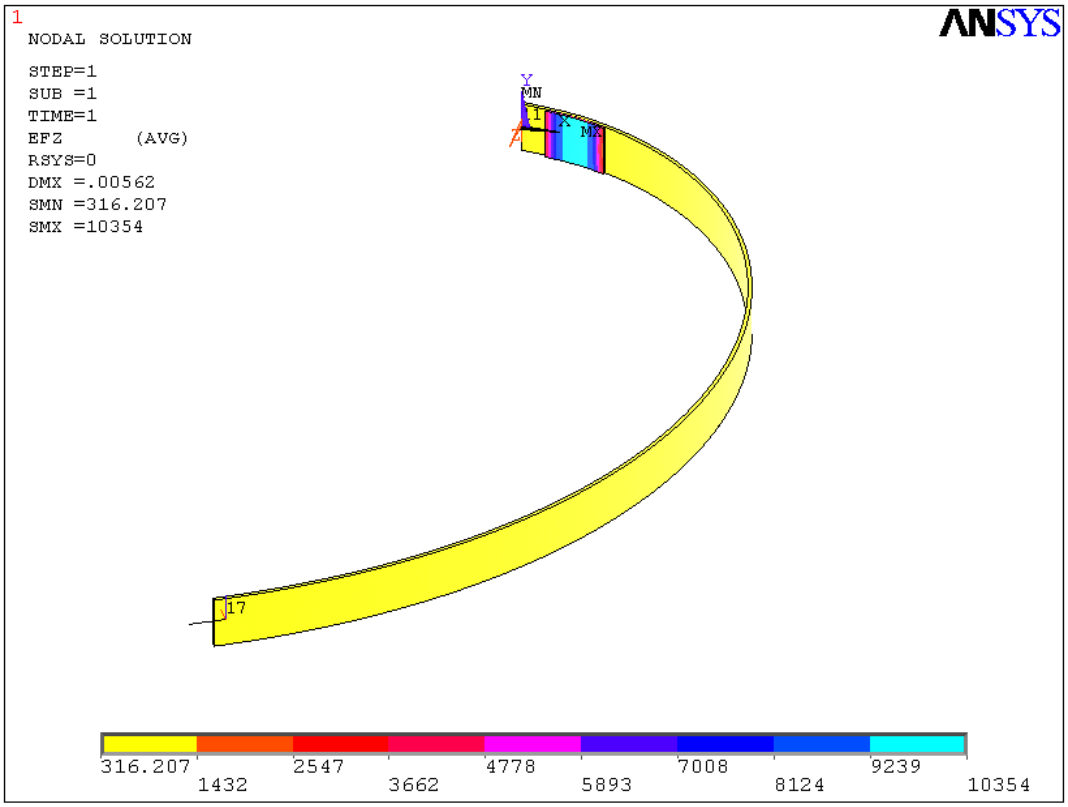

Figure 3.8. Electric field of smart curved beam in *z* direction due to tip load 0.1 N

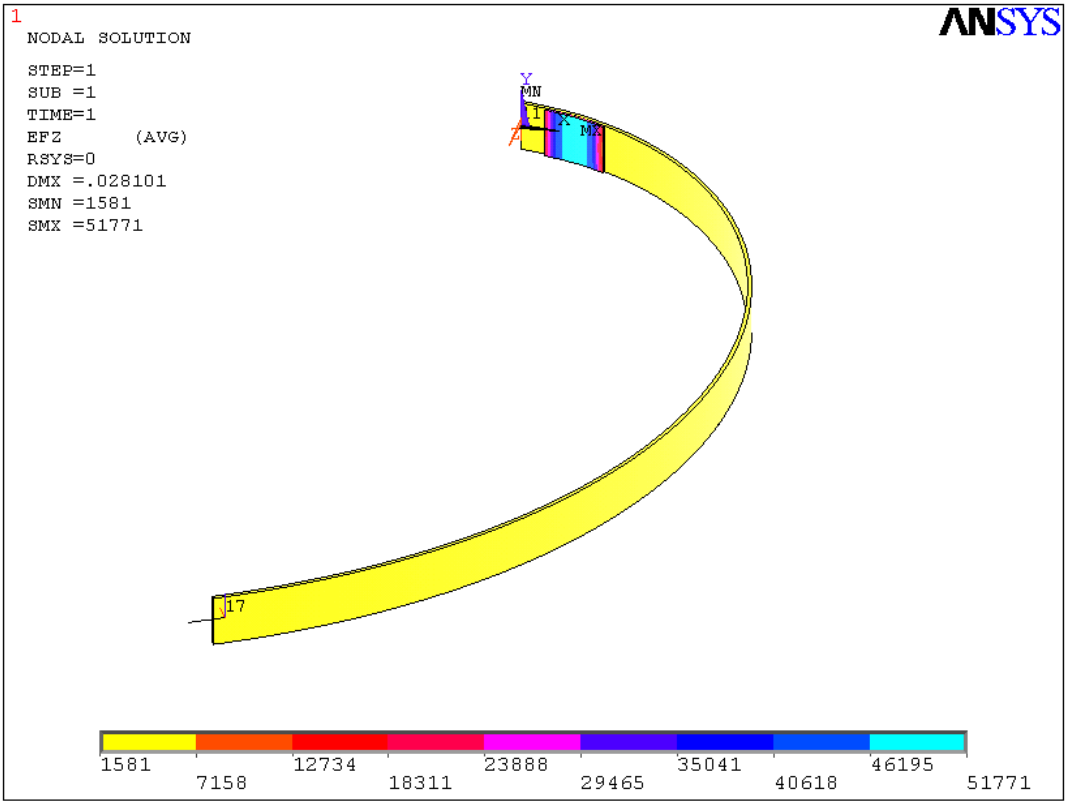

Figure 3.9. Electric field of smart curved beam in *z* direction due to tip load 0.5 N

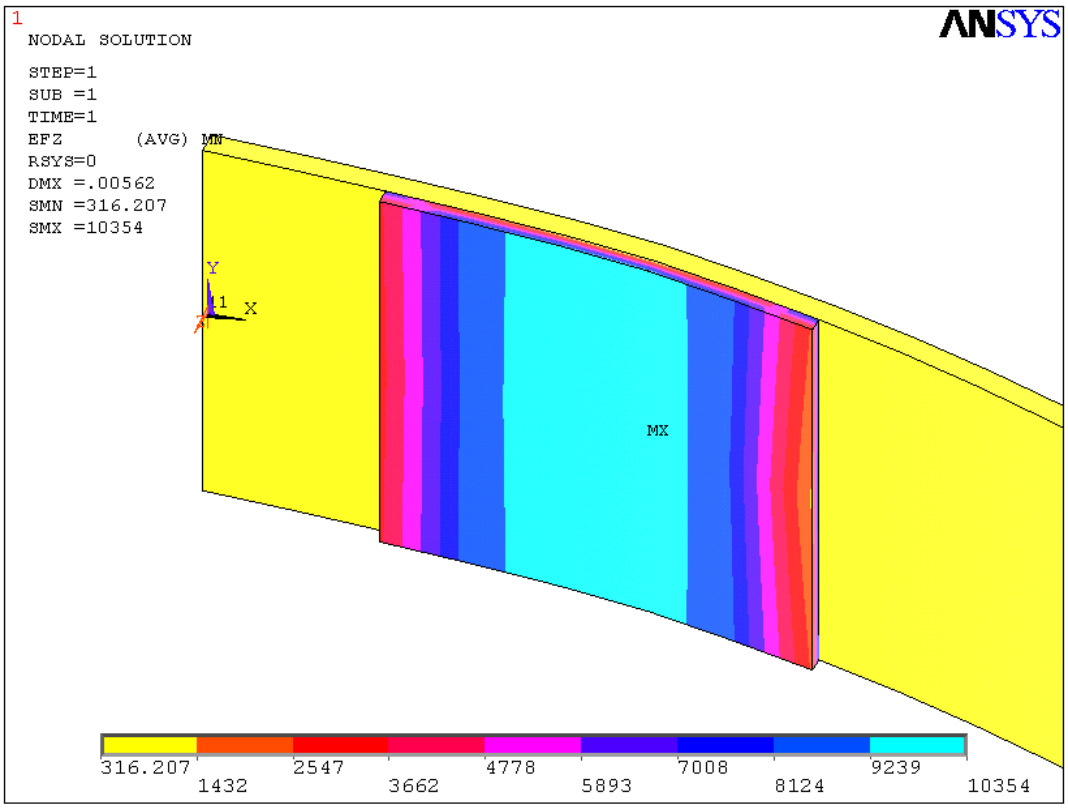

Figure 3.10. Electric field of PZT layer in *z* direction due to tip load 0.1 N

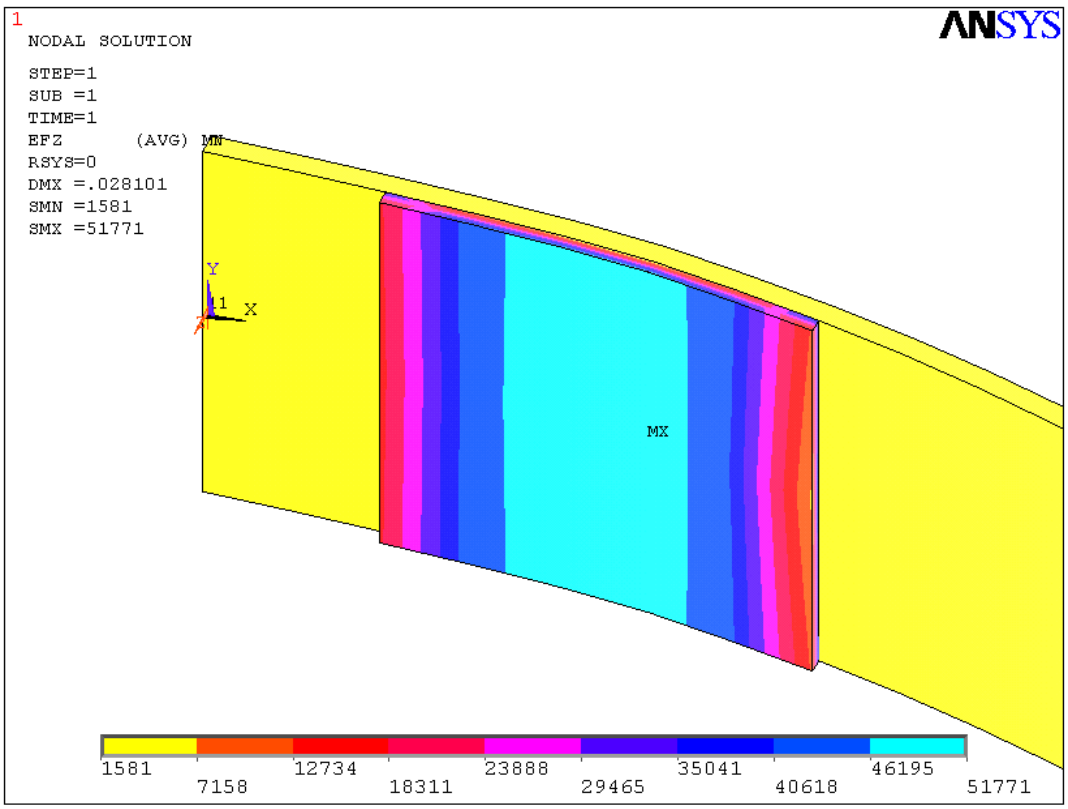

Figure 3.11. Electric field of PZT layer in *z* direction due to tip load 0.5 N

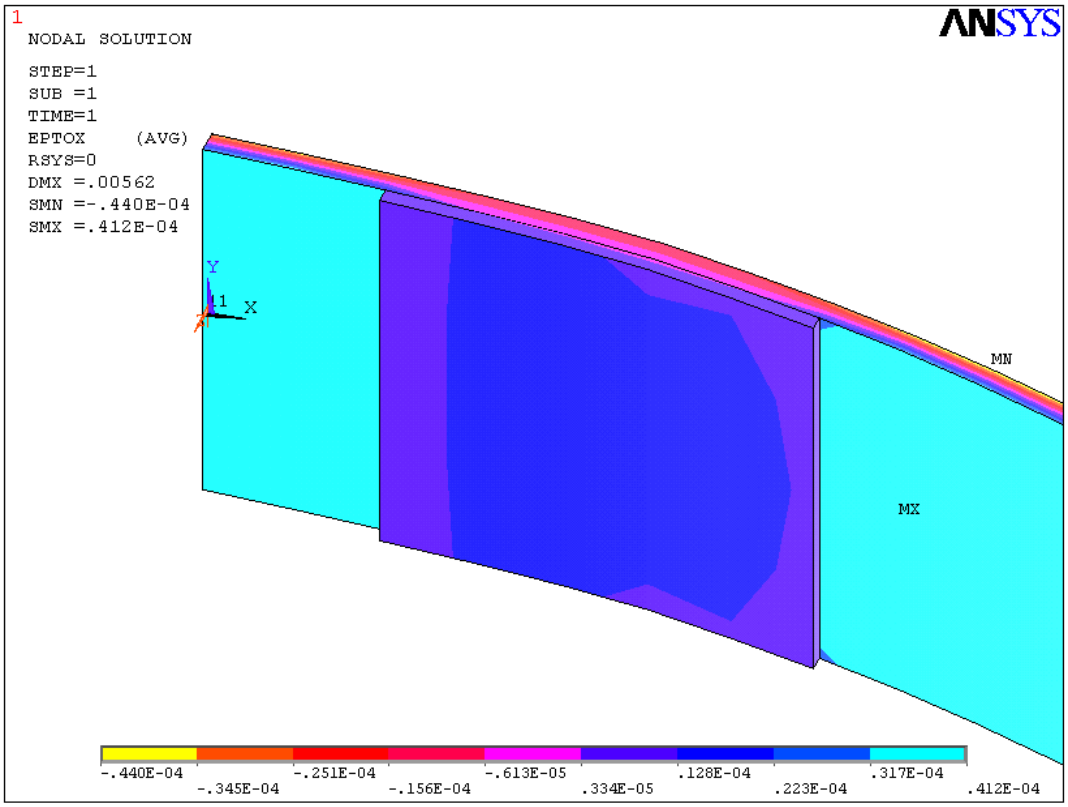

Figure 3.12. Strains of PZT layer in *x* direction due to tip load 0.1 N

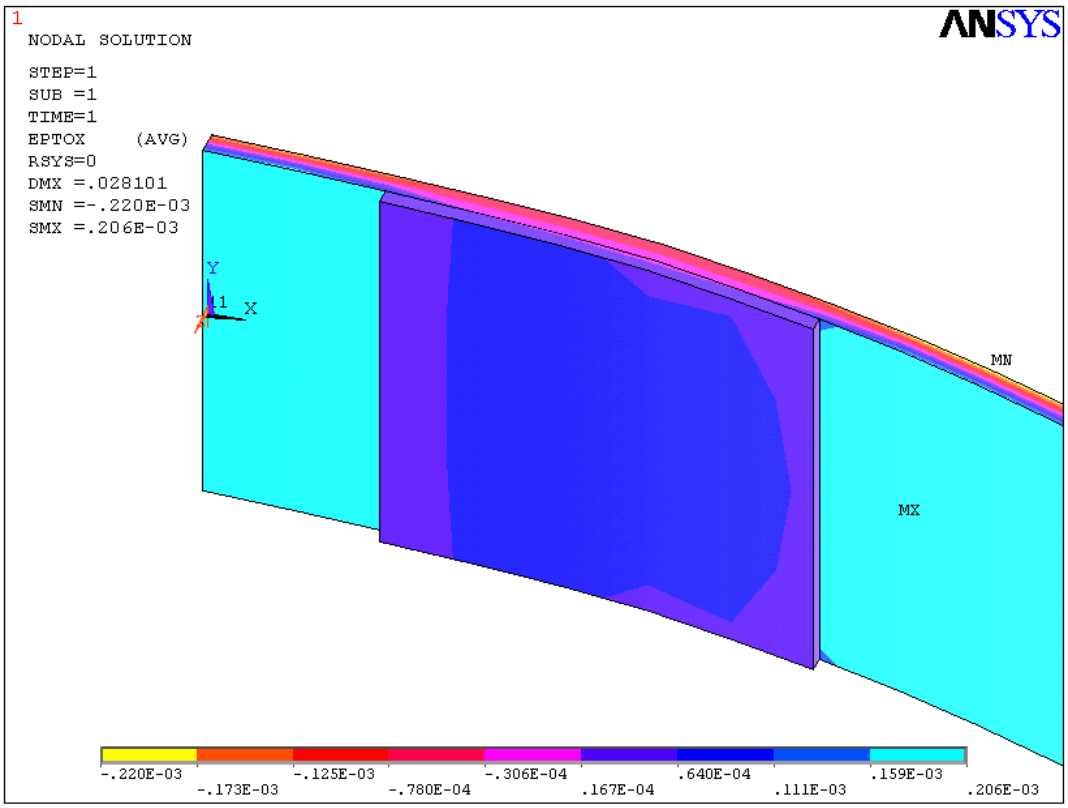

Figure 3.13. Strains of PZT layer in *x* direction due to tip load 0.5 N

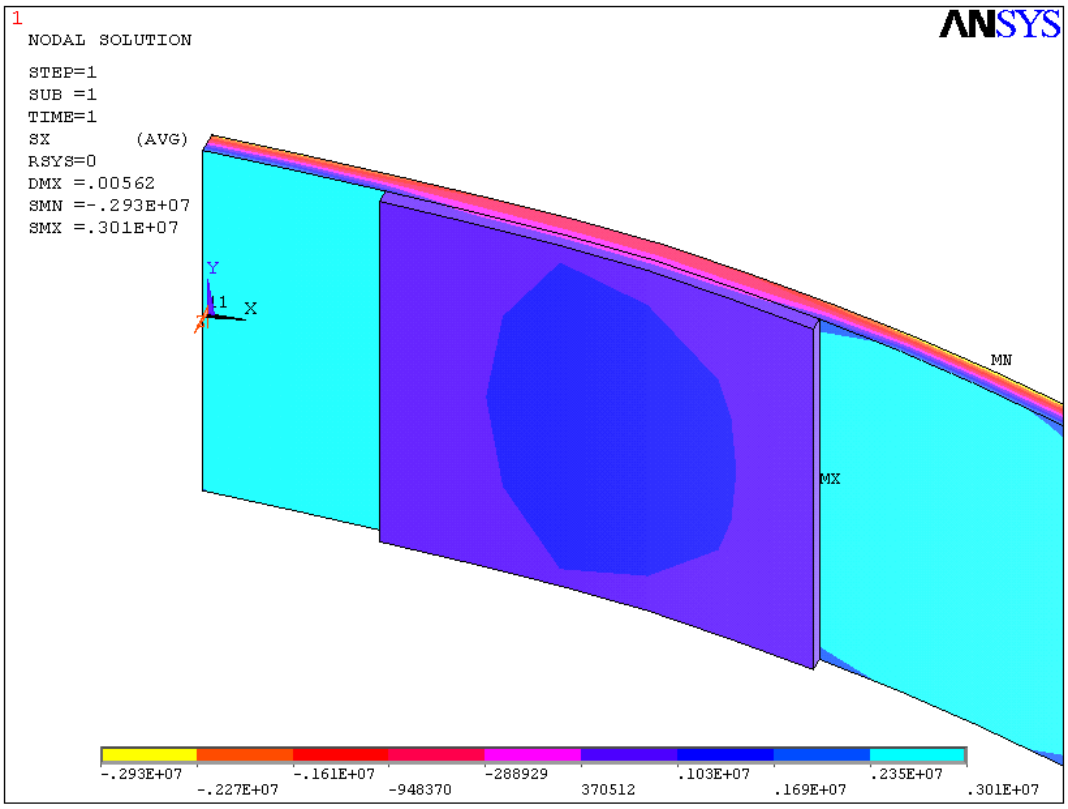

Figure 3.14. Stresses of PZT layer in *x* direction due to tip load 0.1 N

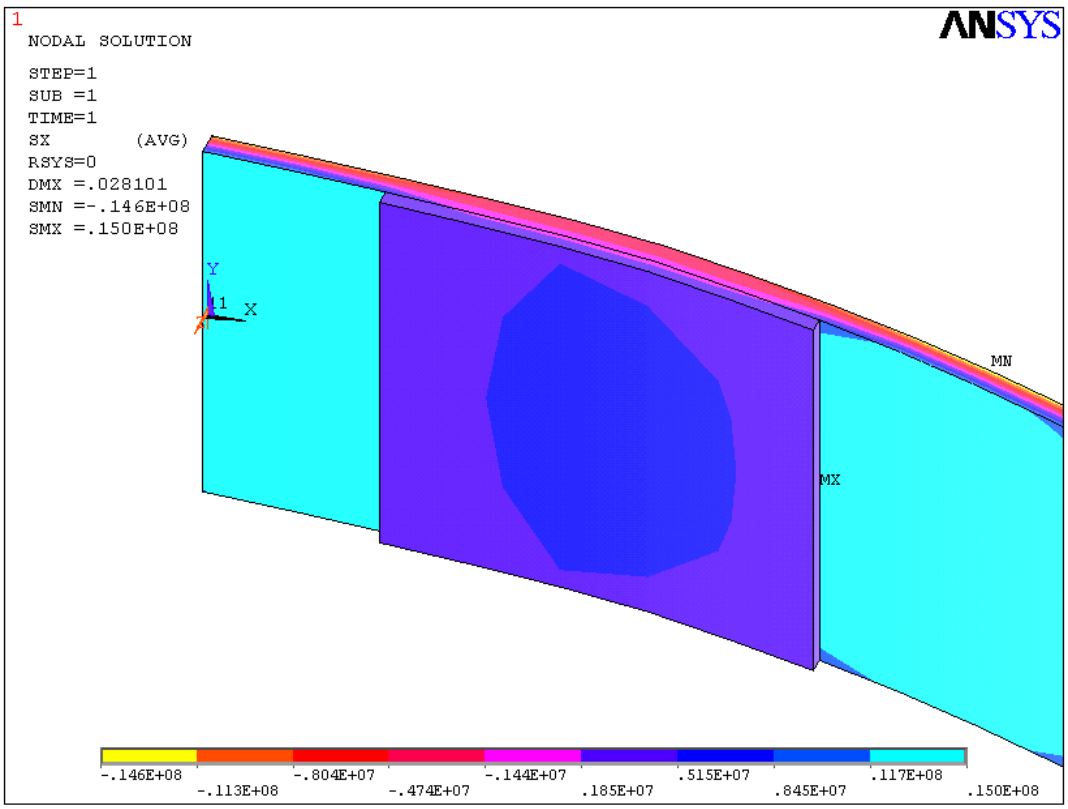

Figure 3.15. Stresses of PZT layer in *x* direction due to tip load 0.5 N

3.3. Discussion of Numerical Results

Electromechanical behavior of the curved beam with PZT layer is analyzed in Section 3.2. Results that were gathered with respect to the different tip load are given in Table 3.4.

Table 3.4. Results comparison for different loadings

	Tip load (N)	
	0.1	0.5
Tip displacement in *x* direction (mm)	0.00562	0.028101
Maximum electric field in *z* direction (V/m)	10354	51771
Maximum strain of PZT layer in *x* direction	2.23E-05	1.11E-04
Maximum stress of PZT layer in *x* direction (Pa)	1.69E+06	8.45E+06

The following statements can be said:

- The highest electric fields which are first part from the right, strains which are third part from the right and stresses which are third part from the right occurred at the middle of piezoelectric patches for both cases. Furthermore, the resultant patterns on the figures did not changed when the load was changed.
- The in-plane displacements of the curved beam under the tip load acting in plane of the neutral axis of the curved beam is obtained linearly proportional to tip load as expected from the linear elasticity.
- Electrical field generated by strains in piezoelectric layer due to the tip load is linearly proportional to tip load again as expected from the theory
- Strains of PZT layer in *x* direction due to tip load are proportional to loading.
- Stress levels in root region of curved beam and PZT layer are proportional to the loading.

CHAPTER 4

CONCLUSIONS

In this study, electromechanical behavior of piezoelectric smart curved beam with variable radius of curvature is investigated using the Finite Element Method.

The voltage generation due to the tip load applied to curved beam can be estimated by using strain values of piezoelectric patches calculated from piezoelectric constitutive equations and mechanics of materials. However, for a curved beam with variable curvature, estimation of the voltage generated by piezoelectric patch is not possible as a circular curved beam. Therefore, a numerical study is necessary to analyze the smart curved beam with variable curvature.

REFERENCES

Allik, H., Hughes, T.J.R., 1970. Finite Element Method for Electric Vibration, *International Journal for Numerical Methods in Engineering* (2): 151-157

Akaydin, H.D., Elvin, N., and Andreopoulos, Y., 2010. Energy Harvesting from Highly Unsteady Fluid Flows using Piezoelectric Materials, *Journal of Intelligent Material Systems and Structures* 21(13): 1263–1278.

Aldraihem, O.J., Wetherhold, R.C., and Singh, T., 1997. Distributed Control of Laminated Beams: Timoshenko Theory vs. Euler-Bernoulli Theory, *Journal of Intelligent Material Systems and Structures* 8(2): 149–157.

Ansari, M.H., and Karami, M.A., 2016. Modeling and experimental verification of a fan-folded vibration energy harvester for leadless pacemakers, *Journal of Applied Physics* 119(9): 94506.

Anton, S.R., and Inman, D.J., 2008. Vibration energy harvesting for unmanned aerial vehicles. International Society for Optics and Photonics, San Diego, California, United States, 692824.

Anton, S.R., and Sodano, H.A., 2007. A review of power harvesting using piezoelectric materials (2003–2006), *Smart Materials and Structures* 16(3): R1–R21.

Bailey, T., and Hubbard, J.E., 1985. Distributed piezoelectric-polymer active vibration control of a cantilever beam, J*ournal of Guidance, Control, and Dynamics* 8(5): 605–611.

Baker, J., Roundy, S., and Wright, P. 2005. Alternative Geometries for Increasing Power Density in Vibration Energy Scavenging for Wireless Sensor Networks. 3rd International Energy Conversion Engineering Conference, San Francisco, California, 5617.

Bauchau, O.A., and Craig, J.I. 2009a. Structural Analysis. Springer Netherlands.

Bauchau, O.A., and Craig, J.I. 2009b. Structural Analysis. Springer Netherlands.

Benjeddou, A. 2000. Advances in piezoelectric finite element modeling of adaptive structural elements: a survey. *Computers & Structures* 76(1–3): 347–363.

Berry, J.I. 1972. Vehicle speed synthesizer. Retrieved from https://www.google.com/patents/US3664711

Bibo, A., Abdelkefi, A., and Daqaq, M.F. 2015. Modeling and Characterization of a Piezoelectric Energy Harvester Under Combined Aerodynamic and Base Excitations. *Journal of Vibration and Acoustics* 137(3): 31017.

Borgen, M.G., Washington, G.N., and Kinzel, G.L. 2003. Design and evolution of a piezoelectrically actuated miniature swimming vehicle. *IEEE/ASME Transactions on Mechatronics* 8(1): 66–76.

Bowen, C.R., and Arafa, M.H. 2014. Energy harvesting technologies for tire pressure monitoring systems. *Advanced Energy Materials* 5(7): 1401787.

Brei, D.E. 1995. Design and development of a new class of piezoelectric actuators for force improvement. Active Materials and Smart Structures, College Station, Texas, United States, 343–356.

Brei, D.E., and Blechschmidt, J. 1992. Design and static modeling of a semiconductor polymeric piezoelectric microactuator. *Journal of Microelectromechanical Systems* 1(3): 106–115.

Bryant, M., and Garcia, E. 2011. Modeling and Testing of a Novel Aeroelastic Flutter Energy Harvester. *Journal of Vibration and Acoustics* 133(1): 11010.

Cain, J.R., Abbott, U.K., and Rogallo, V.L. 1967. Heart Rate of the Developing Chick Embryo. *Experimental Biology and Medicine* 126(2): 507–510.

Cao, J., Wang, W., Zhou, S., Inman, D. J., & Lin, J. 2015. Nonlinear time-varying potential bistable energy harvesting from human motion. *Applied Physics Letters* 107(14): 143904.

Cao, J., Zhou, S., Inman, D.J., and Lin, J. (2015). Nonlinear Dynamic Characteristics of Variable Inclination Magnetically Coupled Piezoelectric Energy Harvesters. *Journal of Vibration and Acoustics* 137(2): 21015.

Challa, V.R., Prasad, M.G., Shi, Y., and Fisher, F., 2008. A vibration energy harvesting device with bidirectional resonance frequency tunability. *Smart Materials and Structures* 17(1): 15035.

Chen, Y.H., Li, T., Boey, F.Y.C., and Ma, J. 2008. Electrophoretic deposition and characterization of helical piezoelectric actuator. *Ceramics International* 34(1): 1–6.

Clair, D.S., Bibo, A., Sennakesavababu, V.R., Daqaq, M.F., and Li, G. 2010. A scalable concept for micropower generation using flow-induced self-excited oscillations. *Applied Physics Letters* 96(14): 144103.

Cottone, F., Vocca, H., and Gammaitoni, L. 2009. Nonlinear Energy Harvesting. *Physical Review Letters* 102(8): 80601.

Cucci, G.R. 1982. Vibrating beam pressure sensor. Retrieved from https://www.google.ch/patents/US4311053

Crawley, E.F., and De Luis, J. 1987. Use of piezoelectric actuators as elements of intelligent structures. *AIAA Journal* 25(10): 1373–1385.

Crownover, J.W. 1962. Piezoelectrical ignition systems. Retrieved from https://www.google.com/patents/US3229154

Dineva, P., Gross, D., Müller, R., and Rangelov, T. 2014. Dynamic Fracture of Piezoelectric Materials SE - 2. Springer, Cham.

duToit, N.E., Wardle, B.L., & Kim, S.-G. 2005. Design Considerations For Mems-Scale Piezoelectrıc Mechanical Vibration Energy Harvesters. *Integrated Ferroelectrics* 71(1): 121–160.

Elvin, N.G., Elvin, A.A., and Spector, M. 2001. A self-powered mechanical strain energy sensor. *Smart Materials and Structures* 10(2): 293–299.

Elvin, N.G., Lajnef, N., and Elvin, A.A. 2006. Feasibility of structural monitoring with vibration powered sensors. *Smart Materials and Structures* 15(4): 977–986.

Erturk, A., and Inman, D.J. 2008. Issues in mathematical modeling of piezoelectric energy harvesters. *Smart Materials and Structures* 17(6): 65016.

Erturk, A., and Inman, D.J. 2009. An experimentally validated bimorph cantilever model for piezoelectric energy harvesting from base excitations. *Smart Materials and Structures* 18(2): 025009.

Ferrari, M., Ferrari, V., Guizzetti, M., Andò, B., Baglio, S., and Trigona, C. (2010). Improved energy harvesting from wideband vibrations by nonlinear piezoelectric converters. *Sensors and Actuators A: Physical*, 162(2): 425–431.

Gautschi, G. 2002. Piezoelectric Sensorics. Berlin, Heidelberg: Springer Berlin Heidelberg.

Glynne-Jones, P., Beeby, S.P., and White, N.M. 2001. Towards a piezoelectric vibration-powered microgenerator. *IEE Proceedings - Science, Measurement and Technology* 148(2), 68.

Gu, L., and Livermore, C. 2011. Impact-driven, frequency up-converting coupled vibration energy harvesting device for low frequency operation. *Smart Materials and Structures* 20(4): 45004.

Haitao, L., Weiyang, Q., Chunbo, L., Wangzheng, D., and Zhiyong, Z. 2016. Dynamics and coherence resonance of tri-stable energy harvesting system. *Smart Materials and Structures* 25(1): 15001.

Hall, S.R., and Spangler Jr., R.L. 1990. Piezoelectric actuators for helicopter rotor control. 31st Structures, Structural Dynamics and Materials Conference, Long Beach, California, 1076.

Han, S.M., Benaroya, H., and Wei, T. 1999. Dynamics of Transversely Vibrating Beams Using Four Engineering Theories. *Journal of Sound and Vibration* 225(5): 935–988.

Harne, R.L., and Wang, K.W. 2013. A review of the recent research on vibration energy harvesting via bistable systems. *Smart Materials and Structures* 22(2): 23001.

Heggie, W.S. 1977 Transducer for measuring injection pressures of diesel engines. Retrieved from https://www.google.ch/patents/US4038868

IEEE, 1988, IEEE Standard on Piezoelectricity, Std. 176-1987, Piscataway, New Jersey: IEEE.

Igarashi, I., and Chiku, T. 1967. Three-dimensional accelerometer device. Retrieved from https://www.google.com/patents/US3304787

Im, S., and Atluri, S.N. 1989. Effects of a piezo-actuator on a finitely deformed beam subjected togeneral loading. *AIAA Journal* 27(12): 1801–1807.

Inman, D.J. 1991. Analytical and Ecperimental Modeling and Control of Flexible Structures. Retrieved from http://oai.dtic.mil/oai/oai?verb=getRecord&metadataPrefix=html&identifier=ADA235523

Jean-Louis, G., Kripke, D.F., Mason, W.J., Elliott, J.A., and Youngstedt, S.D. 2001. Sleep estimation from wrist movement quantified by different actigraphic modalities. *Journal of Neuroscience Methods* 105(2): 185–91.

Kadooka, K., Taya, M., Naito, K., and Saito, M. 2015. Modeling of a corrugated dielectric elastomer actuator for artificial muscle applications. SPIE Smart Structures and Materials + Nondestructive Evaluation and Health Monitoring, San Diego, California, United States, 943020.

Khaligh, A., Peng, Z., and Cong, Z. 2010. Kinetic Energy Harvesting Using Piezoelectric and Electromagnetic Technologies—State of the Art. *IEEE Transactions on Industrial Electronics* 57(3): 850–860.

Kim, H.S., Kim, J.-H., and Kim, J. 2011. A review of piezoelectric energy harvesting based on vibration. *International Journal of Precision Engineering and Manufacturing* 12(6): 1129–1141.

Koconis, D.B., Kollár, L.P., and Springer, G.S. 1994a. Shape Control of Composite Plates and Shells with Embedded Actuators. I. Voltages Specified. *Journal of Composite Materials* 28(5): 415–458.

Koconis, D.B., Kollár, L.P., and Springer, G.S. 1994b. Shape Control of Composite Plates and Shells with Embedded Actuators. II. Desired Shape Specified. *Journal of Composite Materials* 28(5): 459–482.

Koren, H.W. 1949. Application of Activated Ceramics to Transducers. *The Journal of the Acoustical Society of America* 21(3): 198–201.

Kumar, K., and Narayanan, S. 2008. Active vibration control of beams with optimal placement of piezoelectric sensor/actuator pairs. *Smart Materials and Structures* 17(5): 55008.

Krantz, D.G., Belk, J.H., Dubow, J., Hautamaki, C., Mantell, S.C., Polla, D.L., and Zurn, S.M. 1998. SPIE's 7th Annual International Symposium on Smart Structures and Materials, Newport Beach, California, United States, 124-132.

Krantz, D.G., Belk, J., Biermann, P.J., Dubow, J., Gause, L.W., Harjani, R., Mantell, S., Polla, D. and Troyk P. 1999. SPIE's 8th Annual International Symposium on Smart Structures and Materials, Newport Beach, California, United States, 157-164.

Krommer, M., and Irschik, H. 1999. On the influence of the electric field on free transverse vibrations of smart beams. *Smart Materials and Structures* 8(3): 401–410.

Labuschagne, A., van Rensburg, N.F.J., and van der Merwe, A.J. 2009. Comparison of linear beam theories. *Mathematical and Computer Modelling* 49(1–2): 20–30.

Leadenham, S., and Erturk, A. 2014. M-shaped asymmetric nonlinear oscillator for broadband vibration energy harvesting: Harmonic balance analysis and experimental validation. *Journal of Sound and Vibration* 333(23): 6209–6223.

Leadenham, S., and Erturk, A. 2015. Nonlinear M-shaped broadband piezoelectric energy harvester for very low base accelerations: primary and secondary resonances. *Smart Materials and Structures* 24(5): 055021.

Lee, B.S., Lin, S.C., Wu, W.J., Wang, X.Y., Chang, P.Z., and Lee, C.K. 2009. Piezoelectric MEMS generators fabricated with an aerosol deposition PZT thin film. *Journal of Micromechanics and Microengineering* 19(6): 65014.

Lee, C.K., and Moon, F.C. 1990. Modal Sensors/Actuators. *Journal of Applied Mechanics* 57(2): 434.

Lee, G.-S. 1996. System identification and control of smart structures using neural networks. *Acta Astronautica* 38(4–8): 269–276.

Lee, H.-J. 2000. Finite Element Analysis of Individual Curved and Straight Thermopiezoelectric Bimorph Actuators. *Science and Engineering of Composite Materials* 9(3).

Lee, J.K., and Marcus, M.A. 1981. The deflection-bandwidth product of poly(vinylidene fluoride) benders and related structures. *Ferroelectrics* 32(1): 93–101.

Lee, K.A., Portillo, C.J., and Miramontes, H. 2001. The Influence of Sleep and Activity Patterns on Fatigue in Women With HIV/AIDS. *Journal of the Association of Nurses in AIDS Care* 12: 19–27.

Lee, U., Lesieutre, G., Fang, L., Lee, U., Lesieutre, G., and Fang, L. 1997. Safety design concerns of the piezoelectric layer applications for vibration and noise controls. 38th Structures, Structural Dynamics, and Materials Conference, Kissimmee, Florida,1314.

Li, B., Laviage, A.J., You, J.H., and Kim, Y.-J. 2013. Harvesting low-frequency acoustic energy using quarter-wavelength straight-tube acoustic resonator. *Applied Acoustics* 74(11): 1271–1278.

Li, H., Tian, C., and Deng, Z.D. 2014. Energy harvesting from low frequency applications using piezoelectric materials. *Applied Physics Reviews* 1(4): 41301.

Lobontiu, N., Goldfarb, M., and Garcia, E. 2001. A piezoelectric-driven inchworm locomotion device. *Mechanism and Machine Theory* 36(4): 425–443.

Love, A.E.H. 1944. A treatise on the mathematical theory of elasticity. New York: Dover Publications.

Lu, F., Lee, H.P., and Lim, S.P. 2004. Modeling and analysis of micro piezoelectric power generators for micro-electromechanical-systems applications. *Smart Materials and Structures* 13(1): 57–63.

Mackerle, J. 1998. Smart materials and structures - a finite-element approach: a bibliography (1986-1997). *Modelling and Simulation in Materials Science and Engineering* 6(3): 293–334.

Mackerle, J. 2003. Smart materials and structures—a finite element approach—an addendum: a bibliography (1997–2002). *Modelling and Simulation in Materials Science and Engineering* 11(5): 707–744.

Magoteaux, K.C., Sanders, B., and Sodano, H.A. 2008. SPIE Smart Structures and Materials + Nondestructive Evaluation and Health Monitoring, San Diego, California, 692823.

Maha, A., and Pang, S.-S. 2012. Shape Recovery Model of a Curved Beam Using Piezoelectric Actuation. ASME 2012 Pressure Vessels and Piping Conference, Toronto, Ontario, Canada, 227-233.

Malgaca, L. 2007. Integration of active vibration control methods with finite element models of smart structures, Ph.D. Thesis, Dokuz Eylul University, Izmir.

Masana, R., and Daqaq, M.F. 2012. Energy harvesting in the super-harmonic frequency region of a twin-well oscillator. *Journal of Applied Physics* 111(4): 44501.

Mason, W.P. 1939. Piezoelectric apparatus and circuits. Retrieved from https://www.google.com/patents/US2166763

Mateu, L., and Moll, F. 2005. Optimum Piezoelectric Bending Beam Structures for Energy Harvesting using Shoe Inserts. *Journal of Intelligent Material Systems and Structures* 16(10): 835–845.

Maurini, C., dell'Isola, F., & Del Vescovo, D. 2004. Comparison of piezoelectronic networks acting as distributed vibration absorbers. *Mechanical Systems and Signal Processing* 18(5): 1243–1271.

Mindlin, R.D. 1952. Forced Thickness-Shear and Flexural Vibrations of Piezoelectric Crystal Plates. *Journal of Applied Physics* 23(1): 83–88.

Moskalik, A., and Brei, J. 1997. Deflection-Voltage Model and Experimental Results for Polymeric Piezoelectric C-Block Actuators. *AIAA Journal* 35(9): 1556.

Moskalik, A., and Brei, J. 1999. Force-deflection behavior of piezoelectric C-block actuator arrays. *Smart Materials and Structures* 8(5): 531-543.

Narayanan, S., and Balamurugan, V. 2003. Finite element modelling of piezolaminated smart structures for active vibration control with distributed sensors and actuators. *Journal of Sound and Vibration* 262(3): 529–562.

Norris, F. A. 1969. Piezoelectric force transducer. Retrieved from https://www.google.com/patents/US3479536

Olcott, M.D. 2013. Electron: Greek Etymology and Baltic Mythology. San Jose State University SJSU ScholarWorks. Retrieved from http://scholarworks.sjsu.edu/humanities_pub

Pellegrini, S.P., Tolou, N., Schenk, M., and Herder, J.L. 2013. Bistable vibration energy harvesters: A review. *Journal of Intelligent Material Systems and Structures* 24(11): 1303–1312.

Piefort, V. 2001. Finite Element Modelling of Piezoelectric Active Structures. Université libre de Bruxelles. Retrieved from http://scmero.ulb.ac.be/Publications/Thesis/Piefort01.pdf

Preumont, A., 2002. Vibration Control of Active Structures. Second edition. New York: Kluwer Academic Publishers.

Rauch, I.-D.S., and Witter, K. 1976. Device for writing with liquid ink. Retrieved from https://www.google.com/patents/US3950760

Rayleigh, J.W.S., and Lindsay, R.B. 1945. The theory of sound, Dover.

Renaud, M., Fiorini, P., van Schaijk, R., and van Hoof, C. 2009. Harvesting energy from the motion of human limbs: the design and analysis of an impact-based piezoelectric generator. *Smart Materials and Structures* 18(3): 35001.

Rogallo, V.L. 1967. Force transducer. Retrieved from https://www.google.com/patents/US3304773

Roundy, S., Leland, E.S., Baker, J., Carleton, E., Reilly, E., Lai, E., Wright, P.K. 2005. Improving Power Output for Vibration-Based Energy Scavengers. *IEEE Pervasive Computing* 4(1): 28–36.

Royster, L.H. 1970. The flextensional concept: A new approach to the design of underwater acoustic transducers. *Applied Acoustics* 3(2): 117–126.

Saggere, L., and Kota, S. 1999. Static Shape Control of Smart Structures Using Compliant Mechanisms. *AIAA Journal* 37(5): 572–578.

Seeley, C.E., Chattopadhyay, A., and Brei, D. 1996. Development of a polymeric piezoelectric C-block actuator using hybrid optimization technique. *AIAA Journal* 34(1): 123–128.

Shen, D., Park, J.-H., Ajitsaria, J., Choe, S.-Y., Wikle, H.C.I., & Kim, D.-J. 2008. The design, fabrication and evaluation of a MEMS PZT cantilever with an integrated Si proof mass for vibration energy harvesting. *Journal of Micromechanics and Microengineering* 18(5): 55017.

Shen, M.H.H. 1995. A new modeling technique for piezoelectrically actuated beams. *Computers & Structures* 57(3): 361–366.

Shu, Y.C., & Lien, I.C. 2006. Analysis of power output for piezoelectric energy harvesting systems. *Smart Materials and Structures* 15(6): 1499–1512.

Sirohi, J., and Mahadik, R. 2011. Piezoelectric wind energy harvester for low-power sensors. *Journal of Intelligent Material Systems and Structures* 22(18): 2215–2228.

Sirohi, J., and Mahadik, R. 2012. Harvesting Wind Energy Using a Galloping Piezoelectric Beam. *Journal of Vibration and Acoustics* 134(1): 011009.

Söderkvist, J. 1997. Using FEA to treat piezoelectric low-frequency resonators. *IEEE Transactions on Ultrasonics, Ferroelectrics, and Frequency Control* 45(3): 815-823.

Stanton, S.C., McGehee, C.C., and Mann, B.P. 2010. Nonlinear dynamics for broadband energy harvesting: Investigation of a bistable piezoelectric inertial generator. *Physica D: Nonlinear Phenomena* 239(10): 640–653.

Sun, C., Shi, J., and Wang, X. 2010. Fundamental study of mechanical energy harvesting using piezoelectric nanostructures. *Journal of Applied Physics* 108(3): 34309.

Susanto, K., and Yang, B. 2007. Modeling and Design of a Piezoelectric Forceps Actuator for Meso⁄Micro Grasping. *Journal of Medical Devices* 1(1): 30.

Tabesh, A., and Frechette, L.G. 2010. A Low-Power Stand-Alone Adaptive Circuit for Harvesting Energy From a Piezoelectric Micropower Generator. *IEEE Transactions on Industrial Electronics* 57(3): 840–849.

Tang, L., Yang, Y., and Soh, C.K. 2010. Toward Broadband Vibration-based Energy Harvesting. *Journal of Intelligent Material Systems and Structures* 21(18): 1867–1897.

Thurston, E.G. 1953. The Theoretical Sensitivity of Three Types of Rectangular Bimorph Transducers. *The Journal of the Acoustical Society of America*, 25(5): 870–872.

Tzou, H.S. 1989. Development of a Light-Weight Robot End-Effector Using Polymeric Piezoelectric Bimorph. 1989 International Conference on Robotics and Automation, Scottsdale, Arizona, United States, 1704–1709.

Tzou, H.S., and Howard, R.V. 1992. A Piezothermoelastic Shell Theory Applied to Active Structures. Retrieved from http://oai.dtic.mil/oai/oai?verb=getRecord&metadataPrefix=html&identifier=ADA266713

Tzou, H.S., and Zhong, J.P. 1990. Dynamic adaptivity of "smart" piezoelectric structures. 1990 Technical Symposium on Optics, Electro-Optics, and Sensors, Orlando, Florida, United States.

Vaswani, J., Asnani, N.T., and Nakra, B.C. 1988. Vibration and damping analysis of curved sandwich beams with a visoelastic core. *Composite Structures* 10(3): 231–245.

Wang, G.-F., and Feng, X.-Q. 2010. Effect of surface stresses on the vibration and buckling of piezoelectric nanowires. *EPL (Europhysics Letters)* 91(5): 56007.

Wang, J., Shi, Z., Xiang, H., and Song, G. 2015. Modeling on energy harvesting from a railway system using piezoelectric transducers. *Smart Materials and Structures* 24(10): 105017.

Wang, Q.-M., Du, X., Xu, B., and Cross, L.E. 1999. Theoretical analysis of the sensor effect of cantilever piezoelectric benders. *Journal of Applied Physics* 85(3): 1702–1712.

Wang, W.-C., Wu, L.-Y., Chen, L.-W., & Liu, C.-M. 2010. Acoustic energy harvesting by piezoelectric curved beams in the cavity of a sonic crystal. *Smart Materials and Structures* 19(4): 45016.

Wang, X. 2012. Piezoelectric nanogenerators—Harvesting ambient mechanical energy at the nanometer scale. *Nano Energy* 1(1): 13–24.

Wang, Z.L. 2008. Energy Harvesting for Self-Powered Nanosystems. *Nano Res* 1: 1–8.

Weinstein, L.A., Cacan, M.R., So, P.M., and Wright, P.K. 2012. Vortex shedding induced energy harvesting from piezoelectric materials in heating, ventilation and air conditioning flows. *Smart Materials and Structures* 21(4): 45003.

Wente, E.C. 1922. Piezo-electrical voltage indicator. Retrieved from https://www.google.com/patents/US1438974

Williams, W.S., and Breger, L. 1975. Piezoelectricity in tendon and bone. *Journal of Biomechanics* 8(6): 407–413.

Yang, Z., Wang, Y.Q., Zuo, L., and Zu, J. 2017. Introducing arc-shaped piezoelectric elements into energy harvesters. *Energy Conversion and Management* 148: 260–266.

Yoon, H.-S., and Washington, G. 1998. Piezoceramic actuated aperture antennae. *Smart Materials and Structures* 7(4): 537–542.

Yoon, H.-S., and Washington, G. 2000. Analysis and Design of Doubly Curved Piezoelectric Strip-Actuated Aperture Antennas. *IEEE Transactions On Antennas And Propagation* 48(5): 755–763.

Yoon, H.-S., Washington, G., and Danak, A. 2005. Modeling, Optimization, and Design of Efficient Initially Curved Piezoceramic Unimorphs for Energy Harvesting Applications. *Journal of Intelligent Material Systems and Structures* 16(10): 877–888.

Zhou, S., Cao, J., Inman, D.J., Lin, J., Liu, S., and Wang, Z. 2014. Broadband tristable energy harvester: Modeling and experiment verification. *Applied Energy* 133: 33–39.

Zhou, W., Penamalli, G.R., and Zuo, L. 2012. An efficient vibration energy harvester with a multi-mode dynamic magnifier. *Smart Materials and Structures* 21(1): 15014.

Zhou, Y., Dong, Y., and Li, S. 2010. Analysis of a Curved Beam MEMS Piezoelectric Vibration Energy Harvester. *Advanced Materials Research*: 1578–1581.